Power management Systems for Dynamic Positioning Offshore Support Vessels

Artificial Intelligence and Optimization for Shipboard Microgrids

Mehrzadi, Mojtaba

DOI (link to publication from Publisher):
10.5278/vbn.phd.eng.00087

Publication date:
2020

Document Version
Publisher's PDF, also known as Version of record

POWER MANAGEMENT SYSTEMS FOR DYNAMIC POSITIONING OFFSHORE SUPPORT VESSELS: ARTIFICIAL INTELLIGENCE AND OPTIMIZATION FOR SHIPBOARD MICROGRIDS

BY
MOJTABA MEHRZADI

DISSERTATION SUBMITTED 2020

AALBORG UNIVERSITY
DENMARK

POWER MANAGEMENT SYSTEMS FOR DYNAMIC POSITIONING OFFSHORE SUPPORT VESSELS: ARTIFICIAL INTELLIGENCE AND OPTIMIZATION FOR SHIPBOARD MICROGRIDS

Ph.D. DISSERTATION

by

Mojtaba Mehrzadi

AALBORG UNIVERSITY
DENMARK

Dissertation submitted to the Faculty of Engineering and Science at Aalborg University

For the degree of

Doctor of Philosophy in Electrical Engineering

Dissertation submitted: December 20, 2020

PhD supervisor: Professor Josep M. Guerrero
Aalborg University

Assistant PhD supervisor: Professor Juan C. Vasquez
Aalborg University

PhD committee: Associate Professor Zhenyu Yang (chairman)
Aalborg University

Professor Doris Sàez Hueichapan
University of Chile

Associate Professor Ts. Dr. Muzamir Isa
Universiti Malaysia Perlis (UniMAP)

PhD Series: Faculty of Engineering and Science, Aalborg University

Department: Department of Energy Technology

ISSN (online): 2446-1636
ISBN (online): 978-87-7210-861-2

Published by:
Aalborg University Press
Kroghstræde 3
DK – 9220 Aalborg Ø
Phone: +45 99407140
aauf@forlag.aau.dk
forlag.aau.dk

Printed in Denmark by Rosendahls, 2021

CV

Mojtaba Mehrzadi received the B.Sc. degree in Electrical Engineering from Islamic Azad University (IAU) of Iran, at the Department of Engineering and Technology, in 2007, and the MSc Degree in Control Theory & Control Engineering from IAU, Iran in 2012, respectively. He is currently working towards a Ph.D. degree at the Department of Energy Technology, Aalborg University, Denmark. His research interests include the power management system in the hybrid maritime microgrid.

ENGLISH SUMMARY

Recent developments in the marine industry concentrate on using modern technology to apply an innovative strategy for reducing greenhouse gas emissions (GHG) and increasing energy efficiency. Most advanced ships are equipped with electric propulsion, diesel generators to produce power for variable speed propellers, and distribution systems. Furthermore, maneuvering in deep water due to anchor handling limitations such as oil exploration, offshore wind farm, cable, and pipe laying is defined as a high-risk operation. Advanced technology is known as the dynamic positioning system (DPS) to avoid loss of position and compensate for the ship motions induced by sea disturbances during the DP operation (DPS), which is automatically used to control the ship motions desired position. Hence, the DPS applies to compute the power demand and corresponding command forces and direction to each thruster motors to counteract sea disturbances. Inadequate power can reduce DPS execution, loss of station, power failure, and increase fuel consumption and GHG emissions. Therefore, an energy storage system (ESS) is implemented to improve the power system's reliability and stability to prevent the risk of blackout and power system failure. Furthermore, ESS reduces the propulsion torque and power consumption due to the loading of standby generators during the synchronization process, peak power demand in harsh environments, and closed busbar failure. Accordingly, the unpredicted thruster's power demand due to uncertainties and sudden sea forces changes such as wind and wave is forecasted for PMS in the DP ship based on the artificial intelligence (AI) method.

For that reason, to optimum scheduling and operation of dynamic positioning (DP) ship's power demand with the modern propulsion systems, optimization techniques are being applied with the prospect of significant cost savings. To achieve this goal, the knowledge of future power propulsion demand is an essential issue for short-term load estimating depend on sea state changes. Therefore, the accurate power consumption of DPS thrusters is predicted to maintain the ship's position for the power management system (PMS). Then, PMS will receive adequate knowledge concerning DP power demand in the sea disturbance to optimize power generation and economic dispatch between diesel generators (DGs) and ESS. This study proposed a deep learning method for DP ships to predict thruster's power consumption in the environmental disturbances more accurately for PMS, which is considerably used in the shipboard system's operational planning to improve the stability of DP ships.

Predicting DPS's propulsion power request is already a critical issue where PMS's power demand for maneuvering be subject to sea disturbance.

Consequently, unidentified power consumption is forecasted by deep learning techniques relying on nonlinear regressive neural networks for economic dispatching and operational scheduling between generators in sea disturbances. Therefore, the proposed method estimates precise propulsion's power for setting the PMS's ship location to have high performance in operational conditions. This advanced technique exchanges predicted thruster's power demand with DPS and PMS to enhance operational planning, optimize engine performance, and decrease fuel consumption and GHG emissions in different sea circumstances. Hence, the model is expressed as a multi-objective boundary decision making with mixed-integer nonlinear programming (MINLP) optimization problems. The multi-objective function is also determined to appropriately minimize the sum of operational, emissions, and fuel costs.

Moreover, It Should be mentioned that the MINLP and simulation algorithms are performed in the GAMS and Matlab as an advanced modeling system designed for solving optimization problems. Furthermore, the BARON solvers are used to enable the users to connect the capabilities of GAMS as high-level modeling software for solving objective functions with the ability of optimizers. The combination of deep learning techniques and the proposed optimization method in ESS presence is given an excellent engine performance, lowest fuel consumption, and CO2 emissions during maneuvering and operational condition.

DANSK RESUME

Den seneste udvikling i havindustrien koncentrerer sig om at bruge moderne teknologi til at anvende en innovativ strategi til reduktion af drivhusgasemissioner (GHG) og øget energieffektivitet. De fleste avancerede skibe er udstyret med elektrisk fremdrift, dieselgeneratorer til at producere strøm til propeller med variabel hastighed og distributionssystemer. Desuden defineres manøvrering på dybt vand på grund af begrænsninger i ankerhåndtering som olieefterforskning, havmøllepark, kabel- og rørlægning som en højrisikodrift. Avanceret teknologi er kendt som det dynamiske positioneringssystem (DPS) for at undgå tab af position og kompensere for skibets bevægelser induceret af havforstyrrelser under DP-operationen (DPS), som automatisk bruges til at kontrollere skibets bevægelser ønskede position. DPS gælder derfor for at beregne effektbehovet og de tilsvarende kommandokræfter og retning til hver thrustermotor for at modvirke havforstyrrelser. Utilstrækkelig effekt kan reducere DPS-udførelse, tab af station, strømsvigt og øge brændstofforbruget og drivhusgasemissioner. Derfor implementeres et energilagringssystem (ESS) for at forbedre elsystemets pålidelighed og stabilitet for at forhindre risikoen for blackout og strømsystemfejl. Desuden reducerer ESS fremdrivningsmomentet og strømforbruget på grund af belastning af standbygeneratorer under synkroniseringsprocessen, det maksimale effektbehov i barske miljøer og lukket samlesvigtfejl. Derfor forudsiges den uforudsete thruster's krævede kraft på grund af usikkerhed og pludselige ændringer i havkræfter som vind og bølge for PMS i DP-skibet baseret på kunstig intelligens (AI) -metoden.

For at optimere planlægning og drift af dynamisk positionering (DP) skibs kraftbehov med de moderne fremdrivningssystemer anvendes optimeringsteknikker med udsigt til betydelige omkostningsbesparelser. For at nå dette mål er kendskabet til fremtidig efterspørgsel efter fremdrift et væsentligt spørgsmål for kortsigtet belastningsestimering, afhængig af havtilstandsændringer. Derfor forudsiges det nøjagtige strømforbrug af DPS-thrustere at bevare skibets position for strømstyringssystemet (PMS). Derefter vil PMS modtage tilstrækkelig viden om DP-efterspørgsel efter havforstyrrelser for at optimere elproduktion og økonomisk forsendelse mellem dieselgeneratorer (DG'er) og ESS. Denne undersøgelse foreslog en dyb læringsmetode for DP-skibe til at forudsige thrusterens strømforbrug i miljøforstyrrelser mere nøjagtigt for PMS, som i væsentlig grad bruges i skibssystemets operationelle planlægning for at forbedre stabiliteten af DP-skibe. Forudsigelse af DPS's anmodning om fremdrivningskraft er allerede et kritisk spørgsmål, hvor PMS's magtkrav til manøvrering er udsat for havforstyrrelser.

Følgelig forudsiges uidentificeret strømforbrug ved dyb læringsteknikker, der er afhængige af ikke-lineære regressive neurale netværk til økonomisk afsendelse og operationel planlægning mellem generatorer i havforstyrrelser. Derfor estimerer den foreslåede metode præcis fremdrivningskraft til at indstille PMS's skibsposition til at

have høj ydeevne under driftsforhold. Denne avancerede teknik udveksler forudsagt thruster's energibehov med DPS og PMS for at forbedre driftsplanlægningen, optimere motorens ydelse og mindske brændstofforbrug og drivhusgasemissioner under forskellige havforhold. Derfor udtrykkes modellen som en multi-objektiv grænsebeslutning med blandet-heltal ikke-lineær programmering (MINLP) optimeringsproblemer. Den multi-objektive funktion er også bestemt til passende at minimere summen af drifts-, emissions- og brændstofomkostninger.

Desuden skal det nævnes, at MINLP- og simuleringsalgoritmerne udføres i GAMS og Matlab som et avanceret modelleringssystem designet til at løse optimeringsproblemer. Desuden bruges BARON-løsere til at gøre det muligt for brugerne at forbinde GAMS-funktionerne som modelleringssoftware på højt niveau til løsning af objektive funktioner med optimeringsmuligheder. Kombinationen af dyb læringsteknikker og den foreslåede optimeringsmetode i ESS-tilstedeværelse giver en fremragende motorydelse, laveste brændstofforbrug og CO2-emissioner under manøvrering og driftsforhold.

ACKNOWLEDGEMENTS

This Ph.D. thesis has executed during my studies in Energy Technology Department, Aalborg University, Denmark. This work has been carried out from April 1st, 2018, to March 18th, 2021. Furthermore, special thanks to Otto Mønsted and energy technology department funds for the funding of my study abroad in Leibniz Universität Hannover. I want to say my special thanks to my supervisor Professor Josep M. Guerrero, and my co-supervisor, Professor Juan C. Vasquez, for supporting and study at the Center for Research on Microgrids (CROM). Furthermore, I would like to thank Prof Richard Hanke-Rauschenbach from Leibniz Universität Hannover and Prof Chun-Lien Su from Science and Technology University of Taiwan for their collaborations. Finally, my sincere appreciation goes to my brilliant wife and beautiful children for their patience and support during this Ph.D. work.

TABLE OF CONTENTS

TABLE OF FIGURES

CHAPTER 1. INTRODUCTION

1.1 Background of hybrid DP shipboard system

Nowadays, worldwide public interest reduces GHG emissions and a significant factor in the shipboard system's design and operation. Accordingly, the International Maritime Organization (IMO) has issued guidelines to reduce emissions from the maritime segment since 1983. As a result, it improves the ship's electrical system's efficiency and greenness by researching advanced technologies, management strategies, and network architecture. Since 1880 (for example, the ship's first electrical system), the shipboard power system has evolved following international maritime regulations and costs according to the innovative technology. In a real vessel, the electrical power system is a multi-level power grid that typically uses power electronic devices to integrate multiple electromechanical systems with different levels of voltages and waveform values to meet varying power requirements. The ship's power system consists of generators, distribution systems, electric propulsion motors such as propellers and thrusters with driver units. Mobile engines are usually diesel engines that operate in the high-speed medium or range and have a variable or constant speed. Typically, energy efficiency for medium and high-speed diesel engines is limited by approximately 50% in the operational condition. Most of the produced energy is wasted in the atmosphere with a significant amount of harmful emissions and discharged to the environment. Hence, as a maritime authority, IMO has introduced technical guidelines for fueling each type of ship burns to the ship-owners and builders. This series of technical baselines have been established to measure energy efficiency to decrease GHG emissions from vessels. Hence, this technical guideline introduces program management for all ships, such as an energy efficiency strategy for indicating the operation to measure fuel efficiency and a design index that measures new shipbuilding. In a maritime microgrid, the intelligent power management system based on the energy storage system (ESS) for the DC shipboard power system has been introduced in [1],[2].

The importance of using ESS strategies for greener and smarter ships operation has been investigated on [3] that significantly improved the design for zero emissions, fuel-saving, peak shaving, and the spinning reserve of generators. Furthermore, In [3] proposed using the ESS to decrease fuel consumption in offshore vessels equipped with several diesel generators. Therefore, many PMS algorithms have been used based on mixed-integer linear programming (MILP), the heuristic methods for economic dispatch, and optimal unit power generation commitment [4]. The energy-efficient management results illustrate that it can enhance operational efficiency in saving fuel consumption and reducing generator operating hours [5]. A power management strategy for a hybrid dynamic positioning ship is proposed in [6],[7] for the optimal distribution of power flow between the energy sources, containing the battery ESS and generators. Likewise, the energy management optimization strategies for hybrid

power systems in the shipboard system are presented [8]. The simulation results show the ability of such optimization strategies to achieve reduced fuel consumption and emission reduction. Additionally, to descend fuel consumption under the variable loading circumstances, an optimization algorithm is suggested in [9] and analyzes the hybrid shipboard power system [10]. One of the biggest challenges in the marine industry is the operation in deep water that is a costly and risky maneuver.

1.2. Power management system in DP ship

DPS is an advanced technology widely applied in DP ships and other offshore constructions to maintain vessels' position in the operation region. The semi-submerged vessels and other offshore structures in deep water are continuously subjected to sea disturbances such as waves and wind to keep their hydrocarbon fields. Therefore, DP vessels are consumed lots of energy to keep their location instead of adjusting the tension of anchored ships. Most DP ships are used DGs, ESS, and variable speed drivers for keeping the ship position. On the other hand, the worst-case scenarios for DP ships are shutdown during the offshore operation, such as drilling in gas and oil fields, cable and pipe laying, and offshore wind farm platform in rough weather conditions due to loss of power generation. Figure1-1 demonstrates the configuration of a DP drillship power generation and distribution system[11].

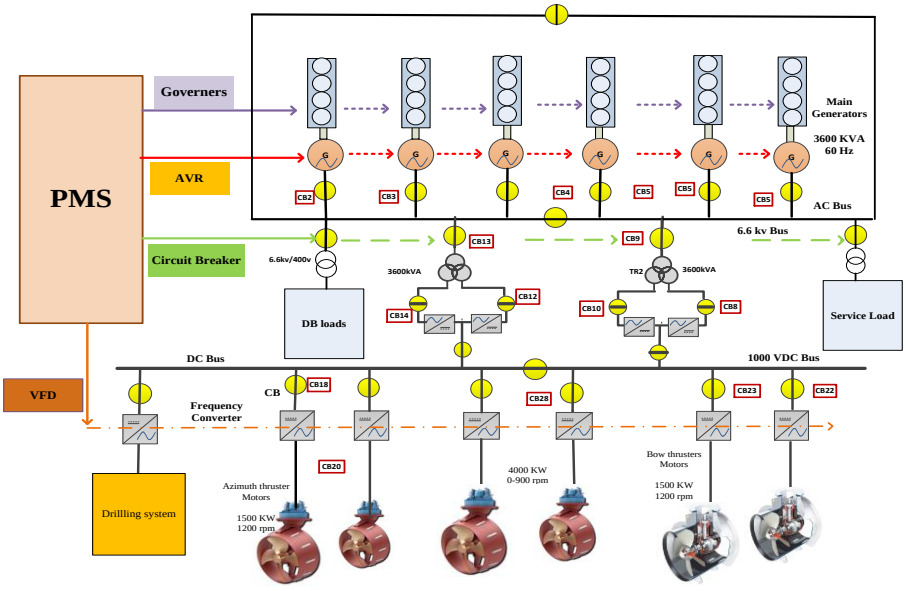

Figure1-1. Configuration of a typical DP ship power generation system and distribution system [11].

The thruster local controllers are adjusted to stabilize the power grid's frequency fluctuations by different commands received from DPS by computing the thrust assignment algorithm (TAA). The thruster's local controller level prevents the probability of the ship's position aberration. In contrast, the individual thrusters controller does not have engagement about the other local controller's performances and cannot calculate the generalized power resultant's deviation. Consequently, thrusters power demands are reduced to compensate for load oscillations on the busbar power plant. Hence, PMS's maximum existing power plant information is used to coordinate the thrusters controller [13]. An essential part of the ability to prevent blackouts is recognized in PMS.

Consequently, ship designers attempt to significantly improve shipboard power systems' stability to prevent blackouts during the DP operation, especially in too rough sea conditions. This project aims to introduce an intelligent control method to avoid the risk of power failure, peak shaving, reduce emissions, fuel consumption. Hence, a deep learning method is used to predict the DP power demand and improve DGs performance with optimal power flow, and economic dispatch of PMS in the presence of ESS, and prediction of thrusters power demand by as shown in the Figure1-2 [13].

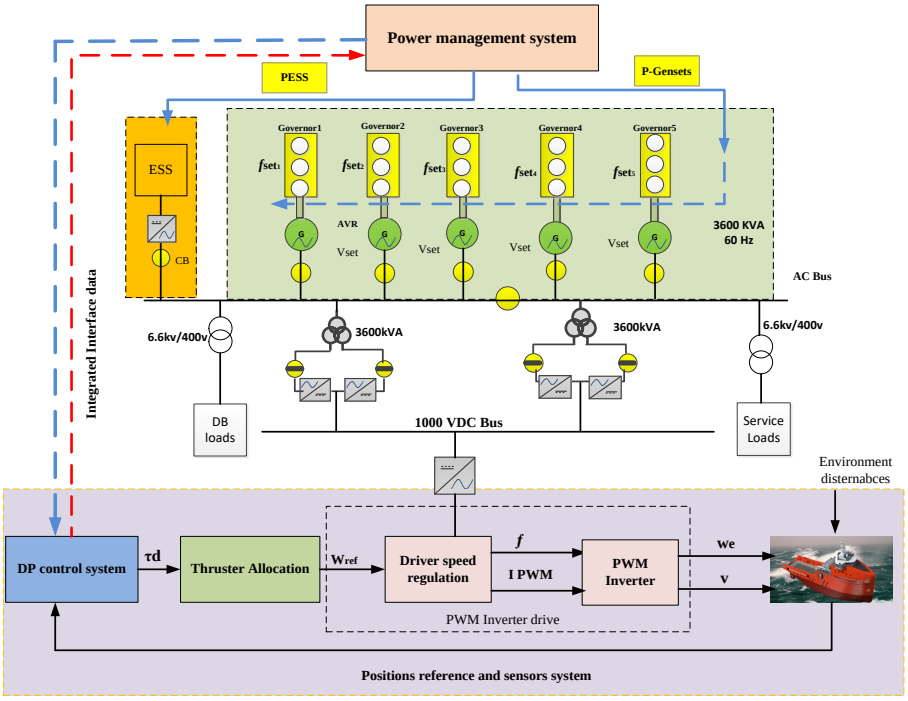

Figure1-2. Configuration of the integrated method with ESS and DP load predicting [13].

1.3. Thesis objectives

- Design and develop PMS by applying the artificial intelligent algorithm for optimal operational planning of generators and ESS based on sea conditions.
- To predict DP power demand precisely by applying machine learning technique for PMS with adequate information to economic dispatch between DGs and ESS in the complexity of DPS's decision-making procedure to keep the ship position in different sea states.
- To investigate the energy storage system's cost-effectiveness to minimize greenhouse gas emissions based on IMO regulations.
- To investigate the accuracy and speed of the power management system's analytical predictions using artificial intelligent control to reduce and synchronize the total number of running hours for all gen-sets.

1.4. Thesis outlines

The outcomes of this Ph.D. thesis are expected to take the form of a collection of relevant published articles throughout the accomplished project period. Furthermore, the Ph.D. thesis is structured as follows:

Chapter 1. Briefly introduces the power management system of dynamic positioning ship background, motivation, research objectives, list of the published journals, and conference papers.

Chapter 2. Introduces the first journal paper where has published in Energies, which reviews the theory of dynamic positioning system and control strategies to achieve advanced control accuracy and decrease ship movement persuaded by the sea disturbances. Furthermore, it studies the possible control techniques and compares the conventional and intelligent controllers in the literature. In addition, this chapter elaborates on the power management system (PMS) in the DP ships as an essential subject for future research.

Chapter 3. This chapter presents deep learning performances in the second paper for the DP load forecasting that is published in applied sciences. In this paper, an iterative nonlinear neural network is used to predict driver power consumption concerning power generation challenges with a comparative degree of accuracy by incorporating climatic parameters' dependences on sea disturbances. The proposed technique forecasts the dynamic load of thrusters in the future more precisely than the traditional PMS methods and enhances the power system's operational planning, and improves the main engine's performance.

Chapter 4. This chapter extends the concept of optimal planning and economic dispatch problems to shipboard systems where some means of generation and storage are also schedulable. The proposed plan's optimal operating strategy is applied to solve the economic dispatch and optimization problems based on the General

Algebraic Modeling System (GAMS) for DP ships. The result shows an efficient PMS solution to optimal power-sharing between DGs and ESS. Accordingly, fuel consumption and greenhouses are significantly decreased by optimal power-sharing.

Chapter 5. This chapter concludes and summarizes the Ph.D. project with the outlook to further investigation.

1.5. List of publications

A list of papers during the Ph.D. study, which is published until now, is given as follows.

Journal Papers

J1. **Mehrzadi, M,** Terriche, Y., Su, C. L., Othman, M. B., Vasquez, J. C. and Guerrero, J. M., "Review of dynamic positioning control in maritime microgrid systems," June 2020, Energies. 13, 12, 3188.

J2. **Mehrzadi, M**, Terriche, Y., Su, C-L., Xie, P., Bazmohammadi, N., N. Costa, M., Vasquez, J. C. and Guerrero, J. M, "A Deep Learning Method for Short-Term Dynamic Positioning Load Forecasting in Maritime Microgrids," July 16th 2020, Applied Sciences.

J3. Terriche, Y, Mutarraf, Muhammad Umair, **Mehrzadi, M**, et al. Adaptive Cascaded Delayed Signal Cancellation-Based Open-Loop Synchronization Technique for Dynamic Response Enhancement of SAPF. Ieee Access, 2019.

J4. Yacine Terriche, Abderezak Lashab 1, Muhammad. U. Mutarraf, **Mehrzadi, M**, et al. "Voltage Stability and Harmonics Mitigation Analyses of Two Effective Compensators for More Electric Marine Vessel Applications," IEEE Transactions on Industry Applications (under review).

J5. Yacine Terriche, Abderezak Lashab 1, Muhammad. U. Mutarraf, **Mehrzadi, M**, et al., "Effective Controls of Fixed Capacitor-Thyristor Controlled Reactors for Power Quality Improvement in Shipboard Microgrids," IEEE Transactions on Industry Applications (accepted for revision).

J6. Peilin Xie, Josep M. Guerrero, Sen Tan, Najmeh Bazmohammadi, Juan C. Vasquez, **Mojtaba Mehrzadi**, Yusuf Al-Turki., "Optimization-based Power and Energy Management System in Shipboard Microgrid: A Review," IEEE system journal (accepted for revision).

Conference

C1. **M. Mehrzadi**, C. Su, Y. Terriche, J. C. Vasquez and J. M. Guerrero, "Operation Planning of Standalone Maritime Power Systems Using Particle Swarm Optimization," *2019 1st International Conference on Electrical, Control and Instrumentation Engineering (ICECIE)*, Kuala Lumpur, Malaysia, 2019, pp. 1-6,

C2. Terriche, Y, Mutarraf, Muhammad Umair, **Mehrzadi, M**., et al. Power quality and Voltage Stability improvement of Shipboard Power Systems with Nonlinear Loads. International Conference on Environment and Electrical Engineering and 2019 IEEE Industrial and Commercial Power Systems Europe (EEEIC/I&CPS Europe). IEEE, 2019. p. 1-6.

C3. Terriche, Y., Mutarraf, M. U., **Mehrzadi, M**., Su, C-L., Guerrero, J. M., & Vasquez, J. C. More in-depth analytical investigations of two Effective Harmonics Filters for More Electric Marine Vessel Applications. *International Conference on Power and Energy Systems (ICPES). IEEE Press, 6 p. 9105508*

C4. Terriche, Y., Su, C. L., Mutarraf, M. U., **Mehrzadi, M**., Lashab, A., Guerrero, J. M., & Vasquez, J. C. (2020, June). Harmonics mitigation in hybrid AC/DC shipboard microgrids using fixed capacitor-thyristor controlled reactors. In *2020 IEEE International Conference on Environment and Electrical Engineering and 2020 IEEE Industrial and Commercial Power Systems Europe (EEEIC/I&CPS Europe)* (pp. 1-6).

CHAPTER 2. DYNAMIC POSITIONING SYSTEM

This chapter summarizes the dynamic positioning system for maritime microgrids published as a review paper in [13]. This chapter's particular consideration is proposed to the relevant issues about the power supply of the thruster's system, and different controllers strategy applied earlier in DP ships.

2.1. Background

In the Marine industry, DPS automatically keeps the location and compensates the ship's motion from the desired position induced by sea disturbances. Due to limitations on anchor handling for offshore operation in deep water, a ship is used propulsion systems such as propellers and thrusters to counteract environmental disturbances. Historically, in the 1960s, a proportional-integral-derivative (PID) was applied in [14] to control ship motion such as sway, surge, and yaw as three degrees of freedom. However, the phase changes in PID control have increased the DP system [15]. Hence, to improve the DP challenges, Balchen and his colleagues were developed the PID controller by the Kalman filtering theory based on the kinematic equations hypothesis [16],[17],[18],[19],[20]. However, the DP system's performance could not be promised due to nonlinear ship motion equations for fixing the position stability and yaw angles. Hence a nonlinear controller based on the backstepping technique was introduced to measure sea disturbance [14].

On the other hand, sea disturbance is dynamic and must be observed to adjust the nonlinear control model parameters. Consequently, a passive nonlinear observer is proposed to reduce the amount of regulating parameters and wave filtering by measuring ship motions' speed containing the low-frequency (LF) position [21]. Therefore, a proportional-derivative (PD) controller is designed to perform the observer filters methodology to remove the noises from the measured ship position and speed, which changes because of sea disturbances. An adaptive nonlinear PID (ANPID) controller was designed in [22] to reduce the ship deflection from setpoint position induced by sea disturbances because of unpredicted position changes. Above and beyond, the (ANPID) has been developed based on adaptive fuzzy logic (AFL) to define nonlinear parameters of the DP controller [23].

Furthermore, to adjust the set of fuzzy rules while the AFL control parameters changes, a neural network (NN) was proposed in [24],[25],[26],[27] to regulate the fuzzy rules and membership. Using the NN for self-tuning member functions in fuzzy logic rules does not consider the mathematical equations in the deriving control model

due to time savings. The obligation of a supplementary study in this field is a hybrid control technique designed in [28] for DP ships to operate from calm to high sea states. The proposed control scheme is analyzed for swapping between nonlinear or linear control in the extreme operating conditions. With the intention of DP controller performance improvement, a model predictive control (MPC) was proposed in [29],[30], and[31] to incorporate the DP system (DPS) and thrusters controller into a single algorithm. The mathematical model of DPS includes environmental changes such as wind, wave disorders, and boundaries input and output of variables. Hence, designing the DPS is typically very complicated because of nonlinearities, uncertainties, instabilities of information, and variable output limitations. The MPC could be performed mathematically in an unidentified system by applying linear models to precisely control a DP ship in the operation zone, as shown in Figure2-1[13].

Additionally, to reduce the mathematical equations' nonlinearities, MPC is a progressive controller to simulate ship motions' future performances through earlier control input consequences, and forecasts appropriate control output response. This proposed method allows the implemented limitations in input and output deviations to forecast the impact of instabilities on the future trend. Thus, the estimation model contains optimization technique abilities for forecasting the DP ship's dynamic response above the defined time perspective. For instance, the study in [32] is presented the MPC model could be effectively performed for DPS, which is dependent on high-superiority control variations in extraordinary restrictions.

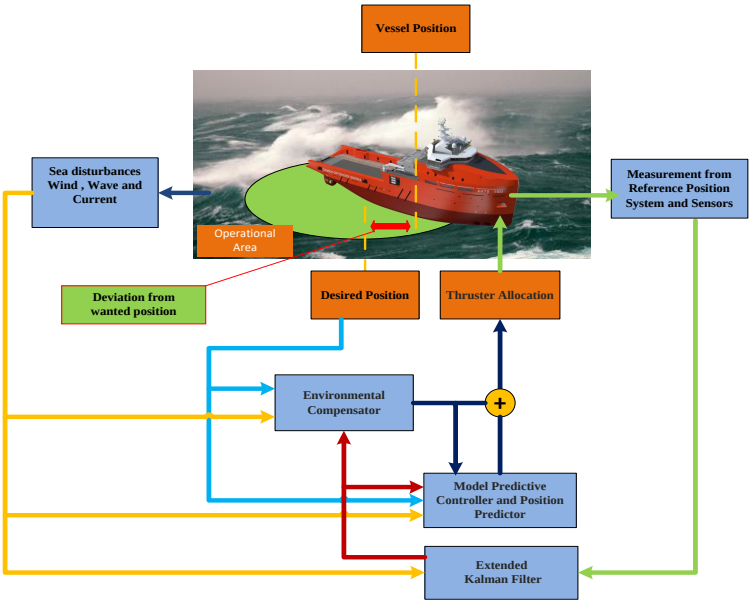

Figure 2-1. The MPC control method for DP ship[13].

On the other hand, the DPS continuously needs a dynamic energy source that thrusters have high priorities to consume power amongst the other heavy consumers on the shipboard [33]. In the DP ships, the grid power typically contains some diesel generators that are connected to the thruster and other consumer connected to the flexible distribution system with different voltage levels and some separable sections. The shipboard system's hierarchical control is distributed through autonomous controllers for DGs fuel oil infusion, generators' magnetization, circuit breaker status, and local and centralized thruster controllers. Undoubtedly, controlling the thruster's power demand based on the desired pitch and rpm setpoint is critical for the PMS to optimally power flow between generators, power failure prevention in the DP ship [7]. The PMS generally has to approve definite changes and report impending oscillations to the maximum available power and TAA energy consumption due to widespread deviation from heavy-duty consumers such as winch, rotary drilling equipment, and offshore wind farm operations [34].

Consequently, the TAA calculates the propulsion power to rotate per minute (RPM) command to regulate thrusters' speed by the related VFD, which power supply is produced from DGs. Additionally, the thruster's controller level makes it possible to predict and limit the deviations of signal errors at the ship's location because the local thrust controllers have no information about each other's execution. As a result, they can not change the generalized power obtained. However, to deal with power fluctuations, local thrust controllers must increase and reduce the requested power allocation. Therefore, PMS regulates local power driver controllers' set points for compensating thruster power fluctuations in shipboard power plants [35].

2.2. DP ship architecture

In many marine operations, fixing the vessel's position and stability is crucial because the ship's position and guidance use continuously dynamic actuators to control environmental forces from waves and winds. Sea disturbances attempt to transfer the vessel from its planned position, so DPS automatically compensates environmental forces and uses its thrusters to keep the vessel stable. A ship's motions have six degrees of independence in the sea, for instance, sway, surge, yaw, which DPS be able to compensate for three horizontal axes and can not control the roll, pitch, and heave of the axis components. A naval ship's mathematical pattern is accurate, such as many physical features to define ship motion observation. Hence, various mathematical models for vessels have been applied and formulated by engineers. Several models of these cases are proposed in [13]and [15], such as the DP ship models and high-speed ships and the phenomenon mathematical of roll parametric resonance. Different features of the ship models are focused on accurately in various operations and different conditions. Typically, the ship's precise model should be designed to contrast the computational and mathematical complexity parameters. Overall, the models that are utilized to build naval ships are more complex than the

schemes that are applied for control objectives. The research in [35] is presented a ship at relatively low speed on the ocean's surface, which the roll, pitch, and heave of the ship motion are not controlled. Hence, the model is used to describe only the flat direction and position of the ship. In a coordinated system, the DP setpoint is determined in the origin of the x-axis directing to the north, y-axis in the east direction, and z-axis directing to the downward based on the right-hand logic [13].

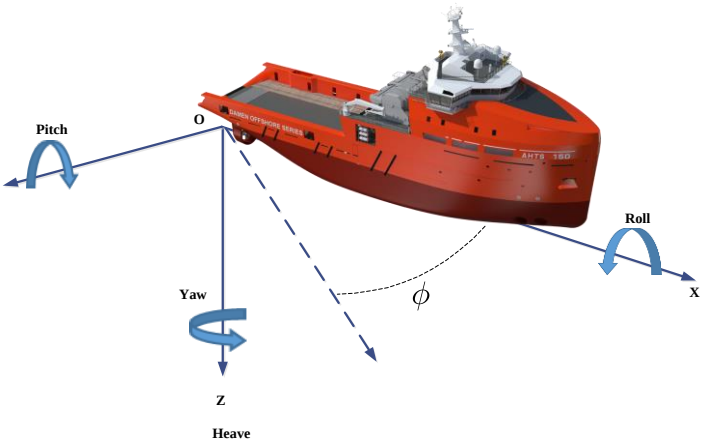

Figure 2-2. The geometrical relationship between the direction and speed of the ship motions [13]

Table 2.1. Abbreviations of velocity and position of the DP ship [13],[36]

Contraction	Description
$\beta = [x\ y\ \phi]^T \in R^3$	Where β is the position and direction of the ship in an inertial structure of the vector x, y, z.
$v = [u_x\ v_y\ r_\phi]^T \in R^3$	Where v is the speed of the ship in its hull frame $u_x\ v_y\ r_\phi$ that is aligned with the vector of $[x\ y\ \phi]^T$.

The direction in which the ship moves horizontally x-y is termed a right-handed rotating with the North reference arc point. The ship's speed is typically defined in its proprietary reference frame as forward speed *u*, lateral speed *v* pointing to the starboard, and the clockwise rotation speed r in the yaw angle direction. The acronym used to define the ship's position and speed is given in Table 1.1, and The geometrical relationship between them is shown in Figure 2-2 [13] and described by [36]:

$$\dot{\beta} = R(\phi)v \qquad (2\text{-}1)$$

where the $R(\phi)$ in [36] and [13] is given:

$$R(\phi) = \begin{bmatrix} \cos(\phi) & \sin(\phi) & 0 \\ -\sin(\phi) & \cos(\phi) & 0 \\ 0 & 0 & 1 \end{bmatrix} \quad (2\text{-}2)$$

2.3. Mathematical Model of DPS

The mathematical model of DP ship has a complicated relationship function, which the hydrodynamics model of vessels is simplified as the first model with the low-reliability[36],[13]. The mathematical model will be the DP controller segment and signified as kinematic development, which separately involves a dynamic ship model. Furthermore, an overview of the actual structure is termed by the second mathematical model as a highly reliable formals model. The real ship's dynamic model is simulated as the mathematical relationship's primary function during the sea disturbances with control inputs and sensor output [36],[13]. Moreover, pitch and roll control models are introduced to compensate for vessels' movement in shallow waters. However, designing and observing control gains might be essential to approximate pitch and roll angular speeds. Nevertheless, the ship's dynamic mathematical model is used in DPS to compute the velocity, acceleration, and location as inputs of the DP controller and adjust the reference points. In [36], the authors are defined in more detail reference models, some local optimization reference point models, and guidance systems.

The majority of ships are equipped with DPS to maintain position utilizing its thrusters force to control the individual thrusters with computers automatically. Therefore, the computer system is designed to compute the different levels of control motion algorithms. The Primary control algorithm is a high-level control motion algorithm that estimates the full moment and force of the thrusters system called the DP control system. At that moment, the TAA synchronizes the thruster's power to supply the requested torque from the DP control system. If the environmental conditions are favorable, the dynamic positioning task's achievement may be negligible. The exact positioning needs of the leisure position are small, and the operator has no concern about fuel and machine wear costs. To control high-level motion, the PID controllers can control three degrees of freedom with a simplistic thrust assigning system. An advanced control algorithm for the high-level motion has been proposed in [32] to rapidly obtain desired positioning and compensate the vessel's deviations via reducing fast changes of thruster's command force restrictions and speed directions. For instance, to control the high-level motion algorithm, an MPC algorithm has been used in [32] to keep the ships within a predetermined operational zone. The typical TAA calculates the allocated command forces of thrusters.

However, in the simulated algorithms, the sea disturbances and ship position limitations for the thrust assigning have not been considered. Recently, most tendencies are concerned with the integrity and increase of the data exchanges through to the thrust assignment and shipboard PMS. Hence, a TAA has been presented in [37] with the range of operations that could be executed equivalency between thrusters power demand and shipboard system to reduce load variations of the power plant.

2.3.1 Dynamic model of the DP ship

The expression of the forces acting on the hull of the vessel is usually the most appropriate. In DPS, the vessel is typically displayed physically rigidly in three degrees of freedom: sway (moving sideways), surge (moving forward), and yaw (vertical rotation around Z-axis). The model is divided into dynamic and kinetic equations where the strengths of the ships and torques come from several physical sources. Hence, the total effect of forces and torque is equivalent to their algebraic sum while the same axis represents the torques. One of the most critical issues to control the DPS is might be the generalized forces produced by thrusters. Other forces acting on a ship consist of hydrodynamic traction, sea currents, and waves. The angular rotational speed of the ship hull orientation is fixed, and the equations of movement typically are improved by Newtonian formulations for centrifugal forces [13]. However, if the yaw angle's rotation speed is moderated, and these conditions can be ignored in this action. An essential component in hydrodynamic traction on the rigid hull of the fluid proportion to the rigid body resists acceleration. Contrasting body mass, the result is not symmetrical, and usually, it is more than longitudinal direction compares with lateral direction for the vessels. Therefore, the obtained equations of motion as a vector are shown as follows [36],[13]:

$$M\dot{v} = -Dv + \tau_{thr} + \tau_{env} \tag{2-3}$$

where M denotes the physical matrix and the mass of hydrodynamic and the generalized mass as follow matrix[36],[13]:

$$M = \begin{bmatrix} m - X_{\dot{u}} & 0 & 0 \\ 0 & m - Y_{\dot{v}} & mx_g - Y_{\dot{r}} \\ 0 & mx_g - N_{\dot{v}} & I_z - N_{\dot{r}} \end{bmatrix} \tag{2-4}$$

Moreover, the estimation value Dv is placed on the right side of this equation changes the signs of the damping matrix elements of D as defined equation in [36],[13]:

$$D = \begin{bmatrix} -X_u & 0 & 0 \\ 0 & -Y_v & -Y_r \\ 0 & -N_v & -N_r \end{bmatrix} \tag{2-5}$$

The environmental forces have not been considered in the Dv and $M\dot{v}$ in (2-3). Therefore, it is proposed as low and high-frequency elements of the wave and wind forces in (2-6) [36],[13]:

$$\tau_{env} = [\tau_{X_{env}} \ \tau_{Y_{env}} \ \tau_{N_{env}}]^T \tag{2-6}$$

where τ_{env} is presented as environmental matrix forces in the direction of the ship motions in the x-y-z axes. The Low-frequency elements of wind and wave forces are controlled by integral operation in the DP controller's algorithm. Typically it is not essential to pay off the wave forces' high-frequency level, where the ship moves forth and back. Before sending position measurements to the DP system, those movements are typically removed by the wave filter. Typically wind force is approximated with wind sensors. In theory, this can be done with sufficient precision, which often faces a tricky situation because of the local changes in the ship's wind velocity and complex geometry. Predicting and modeling of forces is an active research area that is produced by different thruster's device.

2.3.2. Thruster assignment algorithm

The main components of DPS consist of the driver subsystem as essential devices such as main propellers, electronic drive unit, and stern, bow, and azimuths thrusters. The DPS controls the thruster's subsystem to calculate thrust forces and the velocity of propulsion rotation. The high-level controller of thrusters for repositioning the DP ship has been used to forecast the required forces at six degrees of motion. Besides, the thruster assignment algorithm TAA estimates the corresponded thrusters' forces and direct command of each drive motor [36],[13]. To prevent mechanical corrosion parts, harmonious distortion, and blackout in the power supply, the effect of the low-level control of thruster in the calm and rough sea state is emphasized in [38],[13] which the sensors measure the position and speed of the ship motion. As a result, the measured data are transferred for DPS to calculate reference of torque (τd) for high and low levels of thruster control in various marine modes, for instance, extreme rough to slight state correspondingly.

The shipboard power system produces enough power and torque, where the ship's speed is calculated based on position reference by the TAA to bring the vessel to the wanted location. The TAA method calculates the torque τ reference to synchronize the thrusters control command and forces. Therefore, the TAA monitors the torque reference precisely by the slight deviation between the actual and desired generalized

force to improve the transient power fluctuation of the shipboard system. As a result, it is crucial to minimize power reference by applying TAA to decrease power consumption because of momentary deviations from the vessel's position.

2.3.2.1 The resultant force of thrusters

The generalized generated force of i_{th} thruster device is located to the origin of the standard corresponded system, where the generated thruster force f_{ti} at the clockwise angle α_{ti} as from the forward direction is calculated as [36] and [13]:

$$\tau_{ti} = \begin{bmatrix} \cos(\alpha_{ti}) \\ \sin(\alpha_{ti}) \\ -l_{yi}\cos(\alpha_{ti}) + l_{xi}\sin(\alpha_{ti}) \end{bmatrix} f_{ti} \qquad (2\text{-}7)$$

Therefore, the generated generalized force for the entire thrusters system is described in [36] and [13]:

$$\tau_{thr} = T(\alpha_t) f_t \qquad (2\text{-}8)$$

where the thruster configuration matrix columns $T(\alpha_t)$ consist of the TAA that the command force f_t is defined as [36] and [13]:

$$f_t = T^{-1}(\alpha_t)\tau_{thr} \qquad (2\text{-}9)$$

The individual force of thrusters is typically normalized into the range [-1 1]. Furthermore, the desired generalized forces τ_{thr} for all thrusters, which is consist of sway, surge forces, and yaw displacement as the following equation [36]:

$$T(\alpha_t)\, Kf_t = \tau_{thr} + s \qquad (2\text{-}10)$$

The configuration matrix of the general forces $T(\alpha_t)$ generated by individual thruster at the orientation angle vector α_t and the small deviation (s) between the desired thruster's command force and the vessel's actual generalized force $T(\alpha_t)\, Kf_t$ at time *t* is defined in the equation (2-10). The mathematical model does not express the azimuth variations or thruster saturation; hence, the practical application's advanced algorithms are proposed in [36],[13].

2.3.3 Thrusters power consumption and power management system

The power plant capacity must produce sufficient power for the thruster's drive system to keep propeller rotation and torque stationery during the DP operation. The second-ordered estimation is often used to deliver the required power relatively expected to the distributed power square to thrusters. In any situation, the proportion factor between the propeller designs can be very different. In [33], the TAA is proposed to control the thruster system to move away from the directed path to improve the power system's dynamic stability over a short period. The proposed method has been initially studied in [39] to decrease the local thrusters control system's variation. The coordinated deviation from the DP controller commands in the TAA makes it possible to approximate and the boundary deviations due to the ship's speed and position. The minimum power consumption $P_{t\min}$ by the TAA is required to generate the thruster commanded force for solving the nonlinear optimization problem as follows equation [36]:

$$P_{t\min} = \min P_{ct} K \left| f_t \right|^{3/2} + \left\| s \right\|_{q_1}^2 \tag{2-11}$$

where the (2-11) is subjected to (2-8),(2-9) and (2-10) in [36].

$$P_{thr} = P_{ct} K \left| f_t \right|^{3/2} \tag{2-12}$$

The minimum power consumption $P_{t\min}$ by the TAA once the thruster bias power is no obligation in [36]:

$$P_{t\min} = \min P_{ct} K \left| f_t \right|^{3/2} + \left\| K \dot{f}_t \right\|_{\varphi}^2 + C(\dot{P}_{thr} - \dot{P}_{dthr})^2 + \left\| s_2 \right\|_{q3}^2 + \left\| s_1 \right\|_{q2}^2 + \left\| s \right\|_{q1}^2 \tag{2-13}$$

where $\dot{P}_{dthr}$ is specified as the desired change rate of the thruster's power consumption. The proposed signal is used to decrease either power variations or frequency on the shipboard power system. Furthermore, the total power consumption variation cost *C* and the generated variation force resulting from individual thrusters in (2-13) is defined as a quadratic cost matrix φ. Subject to position β_e and velocity v_e deviations of the vessel from the position and speed reference, the boundaries are identified in [36]:

$$-(\max v_e + s_1) \leq v_e \leq (\max v_e - s_1) \quad (2\text{-}14)$$

$$-(\max \beta_e + s_2) \leq \beta_e \leq (\max \beta_e - s_2) \quad (2\text{-}15)$$

Hence, the general thruster command force is allocated to compensate for the variations caused by environmental forces such as waves and wind. The proposed optimization problem in (2-13) consists of individual thrusters' produced force and power consumption variation cost. The solution to minimizing the $P_{t\min}$ is that as long as the deviation between the requested command force τ_{thr} from DPS and the actual generalized force $T(\alpha_t)\,Kf$ situation holds on $S \approx 0$ with the cost matrix q_1 when is useful. The small velocity and position deviation are limited in (2-14) and (2-15) with variables S_1 and S_2 with corresponding cost matrix q_2 and q_3 in (2-13) [36].

Typically PMS confirms some changes and is aware of impending oscillations for current power consumption and maximum available power to TAA due to enormous aberrations from heavy-duty consumers, such as anchor handling, rotary drilling equipment, and cable installation operations. The control command of thruster computes by TAA adjusts the speeds and rotation per minute (RPM) of the thrusters driver, which the power reference generates by the PMS as shown in Figure 2-3 [13]. Moreover, the thruster's driver controller level provides the vision to predict and limit the deviation of signal errors at the ship's position because the local driver controllers have no information on supplementary local controllers' performance. Accordingly, they cannot compute variations in generalized power. However, to manage thrust load oscillations, local driver controllers must increase and decrease power demand. PMS is applied to regulate available generated power for driver controllers [40]. The ability to operate and maneuver ships' position depends on the sea's state and the generator's capacity. Undoubtedly, inadequate power can reduce DP performance, power outages, and positioning, resulting in power outages. The main uncertainty for the DP ship's electrical system is that the thrusters' power under harsh sea conditions can lead to a higher power ratio than the generator's capacity. The excessive DPS power demand for repositioning from distribution units in the DP operating mode will increase the potential of power failure for all types of DP ships. As a result, power systems redundancy is costly due to increasing the power system reliability by using ESS such as batteries, super-capacitors, flywheels, fuel cells, etc. [13].

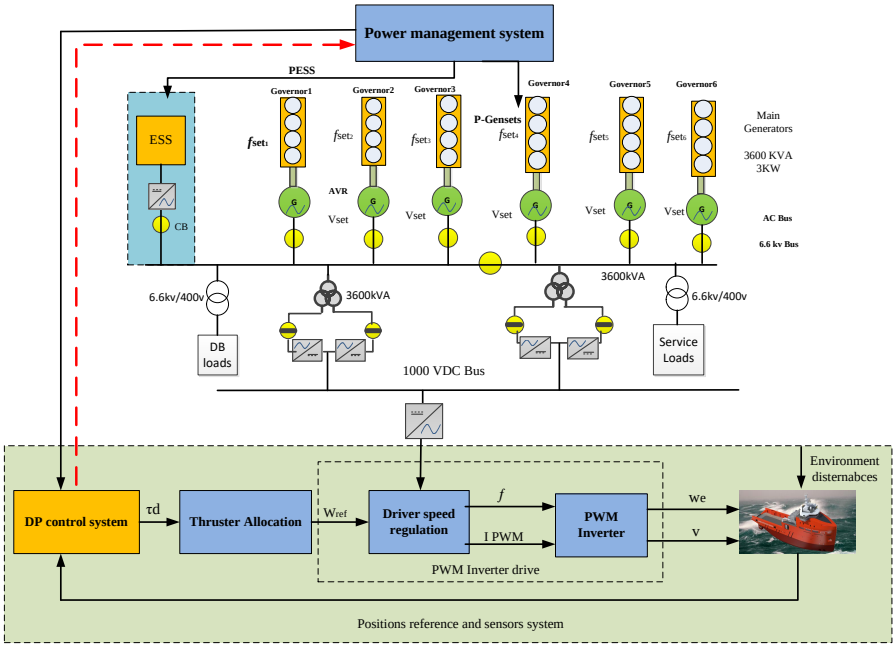

Figure 2-3. Correlation of DPS and PMS control in the DP ship [13].

For example, the shipboard power system's uncertainties due to the DP operation for exploring hydrocarbon resources or transferring energy from offshore wind farms by cable laying are made disturbances in the shipboard system's PMS to provide thrusters command forces [13].

Furthermore, the PMS can control the optimal power-sharing between the generators and ESS during DP operation. Thus, the DP power demand could be estimated by PMS with an effective optimization method [33]. Therefore, power balance flexibility between the DP power demand and power plant production must be appropriate energy resources by applying PMS as a crucial control technique in the marine microgrids [32],[33],[34],[35],[36]. Moreover, energy-efficient and cost-effective solutions are needed to invest in tools, protection, emissions, and fuel consumption due to generator operating hours [9][41]. Hence, the PMS can be sure of DP demand in the prospect of operation conditions and optimal power generations. Along these lines, the requested DP power could be forecast via PMS based on the AI method and efficient optimization strategy [38]. Consequently, the power system stability between the DP demand and power plants is crucial to produce adequate energy resources by performing progressive control methods for PMS in maritime microgrids [10].

CHAPTER 3. DEEP LEARNING FOR DP POWER PREDICTION

This chapter summarizes an intelligent method based on the deep learning algorithm to forecast the requested DP power, which has been published in [38]. The machine learning methodology in this chapter is used to estimate the power thrusters' power consumption in various sea state conditions to increase the power system's stability and reliability in the DP ship operation.

3.1. Introduction

Due to the different character of the proposed controllers, which are reviewed in [13], the control method has been not responding rapidly to unexpected environmental forces changes, for instance, wave and wind storms. At the same time, the station forecast fails to take appropriate and timely action. The DPS compensates for the vessel's movement from the desired position where changing the sea's state affects thrusters' energy consumption in the operational condition. Depending on the high and low-level power consumption of thrusters, the driver speed is increased or reduced correspondingly. Consequently, the setpoint of RPM speed during fast response consumes the full power of power system capacity. In this case, an appropriate driver control command can be used to prevent the shutdown. However, in the rough sea conditions, the driver control must use full power in the bus bar as a high priority to other dynamic power consumers. Otherwise, due to the absence of sufficient energy generated, the thruster control commands cannot stabilize the vessels' position and relocation. The DP system takes power, while the lower steering system calculates each driver engine's corresponding power, speed, and direction. To compensate for the lack of electricity demand, most of these modern ships are utilized generators, shaft generators, and energy storage systems. Inadequate power generations are likely to reduce the lower thruster's efficiency, position, and power failure rates [42].

The main challenge for DP ships is that critical loads, including heavy power requirements for thrusters motor in the rough sea state, may have a greater power consumption inclination than generator power and potentially increase the risk of power outages[35],[43]. To keep away power outages due to the rough sea state, DPS requires to develop via the machine learning algorithm to exchange the predicted DP load profile with PMS to dispatch among the generator-sets and ESS economically[5]. Typically, DPS significantly reduces driver power to prevent dynamic transience in the electrical system. For instance, PMS's unpredicted power demand to conduct DPS in offshore operations increases the power system's instability [35]. PMS is a progressive controller in the shipboard system to determine the optimal power generations giving to DP energy requirements for future operating conditions. Hence, shipboard systems use PMS to control generators and ESS to prevent power outages,

restrictions, load flow, and protection[35]. As a result, DPS manages the available PMS power by applying deep learning techniques to compute thrusters' power consumption in the shipboard power system [38]. Thus, unidentified demand for DP load due to sea uncertainty may impose PMS as an optimization problem [5].

In the marine industry, ship vendors meet numerous economic and technical operational optimization and power system problems. Optimization techniques with essential cost-saving prospects are applied for optimal operation of diesel generators (DGs) for dynamic load and thrusters system [3]. To obtain these objectives, it is very critical to forecasting upcoming power demand in operational conditions. Therefore, predicting the propulsion consumption in different sea states is crucial for optimal power flow between DGs. The load prediction is defined for medium-term load forecast (MTLP), long-term load forecast (LTLP), and short-term load prediction (STLP), which predicts one hour or one day forward [44],[45]. Typically, prediction techniques are used to control generators' power production, distribution, scheduling, planning applications, etc. The STLP is required for economic power dispatching and control of the DP ship's power system, which is applied for fault analysis or power flow distribution [46]. Predicting DP load demand is considered imposes of climate fluctuations on the power network due to thrusters' power consumption. Therefore, a suitable method for DP load forecasting, which depends on sea state and climate changes, is required to investigate this work.

Load forecasting has been performed previously by the Fourier series or trend curve concerning time function. Another method proposed to estimate load performance is an automatic reverting-moving average (ARIMA) [47]. Moreover, the prediction techniques are used to forecast the MTLP model of electricity demand. An automated regression (AR) is a linear approximation method with time and automatic variables for modeling power demand uncertainty. The time series model is described in the ARIMA method, where multiple technique analysis for STLP [48]. For example, the STLP technique based on artificial neural networks (ANN) is applied for extensive data set in [49]. The MTLP-based ANN method is used for past monthly datasets[50]. For adjusting neuron weights for STLP, MTLP, and LTLP based on the fuzzy algorithm, and particle swarm optimization (PSO) method has been used in [51],[52]. In [51], an MTLP has been studied based on the backpropagation (BP) algorithm and analysis features parameters complexity, operation speed, and convergence speed. An ANN-based on fuzzy logic is to analyze and forecast wind speed in [53]. An extensive analysis of wind speed for LTLP is studied in the works of literature [54] and [55] for the nonlinear recurring neural network (NRNN). This work reviews wind speed prediction for electricity demand by applying NN based on automatic regression(ARRX), moving average (ARMARX), and nonlinear automated recurrent with external inputs and (NARX). Moreover, an LM-BP algorithm is used to adjust neurons weight for STLP of wind turbines.

As a result, to optimum power generation between DGs and ESS in DP operation, a recurrent network based on the NN-NARX algorithm is executed to forecast the STLP. Accurate forecasting of DP demand and power estimation is intended to

compensate for ship movement. This method provides the information needed for DP load profiles to make better PMS decisions in marine disturbances. Thus, thrusters' power consumption is anticipated using the correlation method, which is considered an environmentally sensitive load in the shipboard system. To this end, a Levenberg-Marquardt (LM-BP) based on the NARX with environmental disturbances as external inputs is suggested to increase the accuracy of the DP demand for STLP in this research work. The proposed technique is applied to predict hourly, daily, and a month of the thruster's power consumption depending on sea condition. The presented technique's execution is given by collecting real-time DPS parametric data and comparing it with three conventional time series prediction techniques.

3.2. Methodology

The ANN has been progressed significantly because of the ANN's nonlinearity, which can deeply learn from the unidentified environment and estimate NN's properties. The ANN control methods are highly suitable to solve signal processing complexity. The networking model of neurons is categorized as the NN configuration that is designed to predict the real problems of the model. Hence, understanding the DP problem's nature is essential to configure a suitable NN prediction model to solve the DP challenges. Furthermore, the DP operation's reliability and performance are considerably enhanced by assessing the deep learning method's impact.

On the other hand, evaluating NN learning models, structures, and designing algorithms for solving signal processing problems is the most critical issue [56],[57]. Prediction systems based on the ANN method consist of simple neurons and interconnected elements for processing the network's inputs and outputs with actual outputs. Recently, the research of ANN structures is significantly increased since these structures can deliver solutions to some of the problems faced by computer science and artificial intelligence (AI). Figure 3-1 shows an overview of ANN's generalized feedback, commonly used in the ANN structural design.

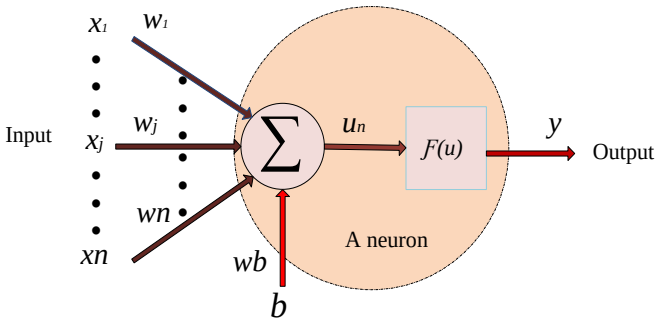

Figure 3-1. Simplified schematic of a neuron [38].

A neuron consists of inputs with varying weights, which changes the network architecture's NN behavior by developing neuron layers and output. The fundamental purpose of changing the NN weight is to execute the anticipated network output. As shown in Figure 3-1, there are n inputs defined $X = [\, x_1 \ldots x_n \,]$ as input matrix-vector correspond to the matrix of weight $W=[\, w_1 \ldots w_n \,]$. The input signals are specified with the bias term b as a constant value, one with the bias weight wb, and the activate function $F(u)$ that can be linear or nonlinear. The multiplied of the sum of the weight inputs, and bias passes via an active function which the NN net function u_n is defined as [38]:

$$u_n = \sum_{i=1}^{n} w_i x_i + wb \times b \qquad (3\text{-}1)$$

The ANN is identified as an entirely interconnected processing array element called neurons. An extensive ANN model that uses multi-neuron networks is a multilayer perceptron (MLP) for the deep learning method [56]. Figure 3-2 displays the ANN feeding of the MLP type, including multi-layered output neurons, multi-input neuron layers, and hidden layers' output.

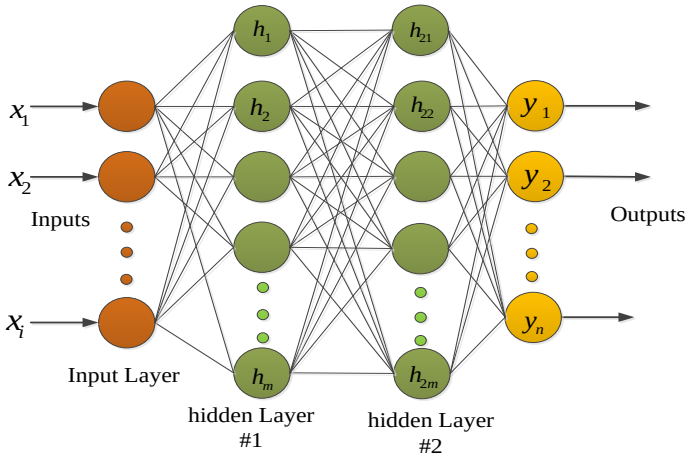

Figure 3-2. A model of MLP configuration with the interconnection of neurons [38].

The inputs layer signal is connected to the output layers with weight and current through the hidden layers to pass over the linear or nonlinear transmission function known as the nonlinear activation function (NAF). In Figure 3-2, a single neuron is symbolized as each circle in the structure. Vertical neuron layers are specified as hidden layers 1 and 2 and connected with different neurons to the output layers. The MLP performs mathematically nonlinear prediction via sigmoid functions [38] as

hidden parts and linear weight in the feedforward NN. The neuron vector feature's weight is continuously modified to decrease the predicted network's signal error and the desired output. Accordingly, equation (3-2) defines the output layers based on multi hidden layer neurons [38]:

$$y_n = \frac{1}{1+\exp[-(w_{bk} + \sum_{j=1}^{m} w_{jk} h_j)]}; 1 \le n \le n \qquad (3\text{-}2)$$

where the input neuron x_i is connected to hidden layer neurons h_i via weights w_{ij} and the output neurons y_i via weights w_{jk}. The hidden-layers neuron is calculated in (3-3), where the input signal passes the summed signal through to the sigmoid function $f(u) = \frac{1}{1+e^{-u/t}}$ in [38]. Therefore, the hidden layers are computed as follow [38]:

$$h_j = \frac{1}{1+\exp[-(w_{bj} + \sum_{i=1}^{l} w_{ij} x_i)]}; 1 \le j \le m \qquad (3\text{-}3)$$

3.2.1 MLP backpropagation learning technique

The training method in multilayer perceptron consists of hidden layers is very complicated. An effective strategy for regulating the MLP neurons' weight is the propagated technique. The single-layer MLP configuration includes a single neuron to provide a replication training method is displayed in Figure 3-3. Accordingly, a neuron is separated into two parts, where the first part summarizes the function of neuron output defined as u and the second section calculates the NAF [38].

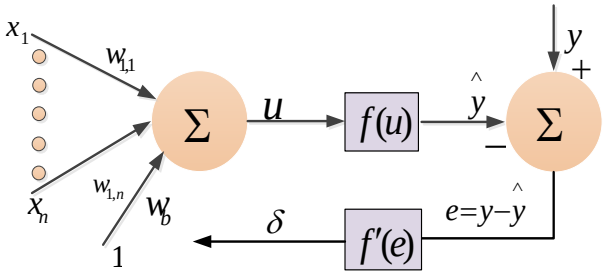

Figure 3-3. MLP training model for a single neuron [38].

The network $\hat{y}$ output is evaluated with the error signal $e = y - \hat{y}$ to calculate deviation from the actual output *y*. The error backpropagation (BP) signal δ is defined for training the input's weight among the MLP network. Therefore, the preliminary estimation for the matrix of weights vector is presented by the square error summation as follows [38]:

$$E_b = \sum_{n=1}^{n} [e_b(n)]^2 = \sum_{n=1}^{n} [y(n) - \hat{y}(n)]^2 = \sum_{n=1}^{n} [y(n) - f(wx(n))]^2 \tag{3-3}$$

where the error square E_b in (3-3) adjusts the matrix of weights (w) to reduce the error signal between actual and network outputs. These adjusted weights matrices are defined as [38]:

$$w_i(t+1) = w_i(t) + \Delta w_i(t) \tag{3-4}$$

Hence, the adjusted weight $w_i(t+1)$, the parameter of current weight $w_i(t)$, and the different weight values $\Delta w_i(t)$ at time *t* in the BP method are defined as the adjusted weight parameter. Equation (3-3) is described as a mean squares error (MSE) optimization problem. Therefore, to minimize the error square E_b, the weights vector-matrix is adjusted in the equation (3-4). Then, to solve the optimization problem of MSE, the gradient descent (GD) set of rules adjusts the weight of neurons related to the BP error signal δ. The quantity E_b of scalar derived in the case of discrete weights is defined as the following equations [38]:

$$\frac{\partial E_b}{\partial w_i} = \sum_{n=1}^{n} \frac{\partial [e_b(n)]^2}{\partial w_i} = \sum_{i=1}^{i} 2[y(n) - \hat{y}(n)](\frac{-\partial \hat{y}(n)}{\partial w_i}) \tag{3-5}$$

where [38]

$$\frac{\partial \hat{y}(n)}{\partial w_i} = \frac{\partial f(u)}{\partial u} . \frac{\partial u}{\partial w_i} = f'(u) \frac{\partial}{\partial w_i} \sum_{i=1}^{n} w_i x_i + w_{nb} = f'(u) x_i \tag{3-6}$$

hence [38]

$$\frac{\partial E_b}{\partial w_i} = -2 \sum_{n=1}^{n} [y(n) - \hat{y}(n)] f'(u(n)) x_i(n) \tag{3-7}$$

Therefore, equation (3-8) calculates as [38]:

$$\frac{\partial E_b}{\partial w_i} = -2\sum_{n=1}^{n} \delta(n) x_i(n) \qquad (3\text{-}8)$$

where the derivative activation function $f'(e)$ reduces the error signal $\delta(n)$. As a result, the global weight changes in (3-4) is adjusted as [38]:

$$w_{ij}(t+1) = w_{ij}(t) + \eta \sum_{n=1}^{n} \delta(n) x_i(n) \qquad (3\text{-}9)$$

For adjusting the weights of MLP, the new symbols are assumed for separate neurons in different layers where the outputs of the earlier neurons are passed the synaptic weights of the *ith* neuron of the *lth* layer as displayed in Figure 3-4 with their related output of learning term [38].

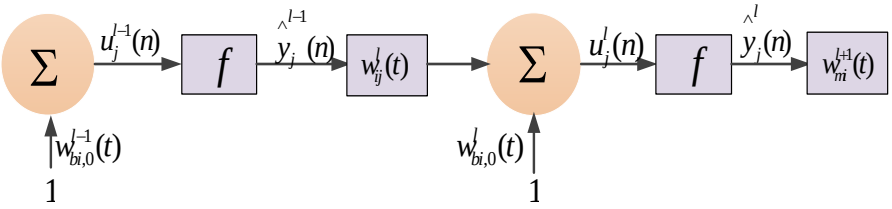

Figure 3-4. The architecture of a typical MLP network [38].

Therefore, GD's produced a set of rules that adjusts the weight's values regarding gradient error (GE) and can be expressed as [38]:

$$\frac{\partial E_b}{\partial w_{ij}^{\ l}} = -2\sum_{n=1}^{n} \frac{\partial E_b}{\partial u^l{}_i(n)} \cdot \frac{\partial u^l{}_i(n)}{\partial w_{ij}^{\ l}} = -2\sum_{n=1}^{n} [\delta_i^l(n).\hat{y}(n)^{(l-1)}] \qquad (3\text{-}10)$$

Equation (3-11) is defined as a BP formula that computes the GE of the output layer and backward to the input layers via passing the hidden layers to regulate the neuron weights. Consequently, delta error $\delta_i^l(n)$ can be an iterative process to compute the $\delta_m^{l+1}(n)$ in the layer weights of $(l+1)th$ where $\hat{y}(n)_i^l$ is overtaken $(l+1)$ *th* layer of the *m* neurons numbers.

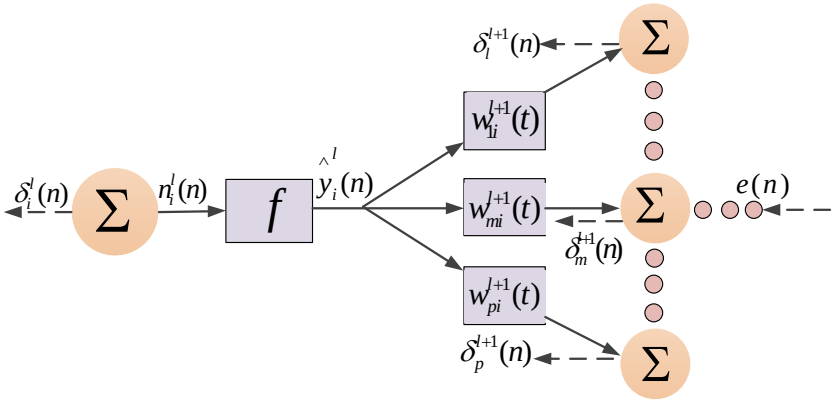

Figure 3-5. The MLP error BP method [38].

The signal error is adapted via the following formulations as [38]:

$$\delta_i^l(n) = \frac{\partial E_b}{\partial u_i^l(i)} = f'(u_i^l(n)).\sum_{m=1}^{M} \delta_m^{l+1}(n).w_{mj}^l \qquad (3\text{-}11)$$

where the adjusted neuron weight in the $(l + 1)th$ layer weights is defined as the last weight changes [38]:

$$w_{ij}^l(t+1) = w_{ij}^l(t) + \eta.\sum_{n=1}^{n} \delta_i^l(n)\,\hat{y}_j^{l-1}(n) + \mu[w_{ij}^l(t) - w_{ij}^l(t-1)] + \varepsilon_{ij}^l(t) \qquad (3\text{-}12)$$

where μ and η are known the continuous momentum constraint and the learning coefficient, respectively. The gradient of the mean square, momentum term, and minor random noise rate is defined to decrease error by adapting the weight values and NN learning algorithm as the second and the third term of the equation (3-12) [38].

3.2.2 Load prediction based on NARX-LM-BP method

In many applications, recurrent learning procedures are not performed online, and they are used offline. In the following sections, the error signal values of NARX are reduced by the LM-BP method [38]. Consequently, due to the improving accuracy of the NARX model during the learning procedure, a history of sea disturbances correlation is performed between input and output. As a result, a NARX-LM method is proposed to forecast the thrusters' power demand as a sensitive load depends on

different sea conditions. The principal mathematical relation for the LM-BP-NARX process in the nonlinear time series pattern is identified in [38],[58], and [59]:

$$y(n,t) = f\left(x(n,t-1),\ldots,x(n,t-Td_x), y(n,t-1),\ldots,y(n,t-Td_n)\right) \qquad (3\text{-}13)$$

where $y(n,t)$, $x(n,t)$, and $f(x)$ shows *kth* output and inputs values and nonlinear activation function, correspondingly. Moreover, the tapped delay lines (TDL) in equation (3-13) are defined as integer numbers of the input and output Td_x and Td_y in RNN, respectively [60]. As a result, the $y(n,t)$ is computed regarding the initial values of the TDL input and output. To calculate the NARX feedforward output, a sigmoid NAF is used as *f(x)* for the learning procedure related to DP power demand. Figure (3-6) is shown, a feedforward series-parallel architecture connected to the NARX input and output preceding values [61].

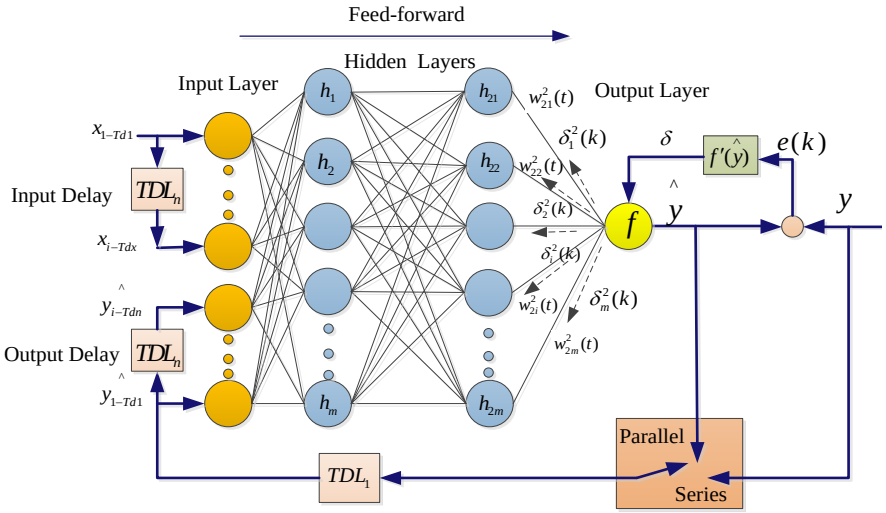

Figure 3-6. The structure of NARX network with BP error and TDL values Tdx and Tdy [38]

As a result, the current output signal in (3-13) is defined based on ambient turbulence related to the signal of the external inputs' previous values such as sea disturbances and DP demand as the output target. In addition, the NARX output mathematical model is computed as [38], [58], and[59]:

$$\hat{y}(n,t) = \hat{f}_{out}\left(\hat{W}_{out}\left(f_{hid}\left(W_{hid}\left(x(n,t-1),\ldots,x(n,t-Td_x), y(n,t-1),\ldots,y(n,t-Td_n)\right)+b_{hid}\right)\right)+b_{out}\right) \qquad (3\text{-}14)$$

where $\hat{y}(n,t)$, $\hat{f}_{out}$, $\hat{W}_{out}$, b_{hid}, and b_{out} are the estimated value of the output, active function, hidden layers, and output bias of weights matrix, respectively. Furthermore, the weight matrix W_{hid} and f_{hid} are the activate function of the hidden layers, respectively. The LM-BP algorithm in [38] is applied for solving the BP scale factor problem, tends to reduce frequently the local error converge in the preference of the total error. Furthermore, BP's performance has been appropriated on the simple learning problem; In contrast, BP's performance is decreased by data-sizing, data quantity growth, and complexity. As a result, BP cannot carry out irregularly, and for DP demand forecasting, the environmental disturbances are recognized as a similar problem.

3.2.3 DP Load forecasting and training method

A real-time data set have been used to forecast the DP demand based on proposed RNN to train, validate, and test the NARX network to predict the DP power request in operation conditions [38]. As a result, to evaluate the proposed method, data sets have been gathered from the load profile of a real DP ship included a weather forecast based on the Caspian sea state in January 2020. Furthermore, the weather parameters that affect thrusters' power consumption due to ship movement from the desired position, such as wind speed and direction, wave height, and wave, are displayed in Table 3-1 and Figure 3-7. The optimization problem and optimal dispatch between generators and ESS in different sea circumstances are solved based on hourly weather changes and predicted DP power demand in PMS. Therefore, the average hourly data sets have been recorded each 2-min in the auto logging system in the DP operation period.

Table 3-1. Parameters applied in LM-BP-based NARX [38].

Descriptions	Parameters		scales
DP power (MW)	$y(n,t)$	DP_L	[0–7]
wave height (m)	$x_1(n,t)$	$W_{h1}(n,t)$	[0–8]
wave deg (Θ)	$x_2(n,t)$	$W_{V2}(n,t)$	[0–360]
wind speed (m/s)	$x_3(n,t)$	$W_{S3}(n,t)$	[0–20]
wind deg (Θ)	$x_4(n,t)$	$W_{D4}(n,t)$	[0–360]
motion deg (Θ)	$x_5(n,t)$	$D(n,t)$	[0–360]
yaw deg (Θ)	$x_6(n,t)$	$H(n,t)$	[0–360]

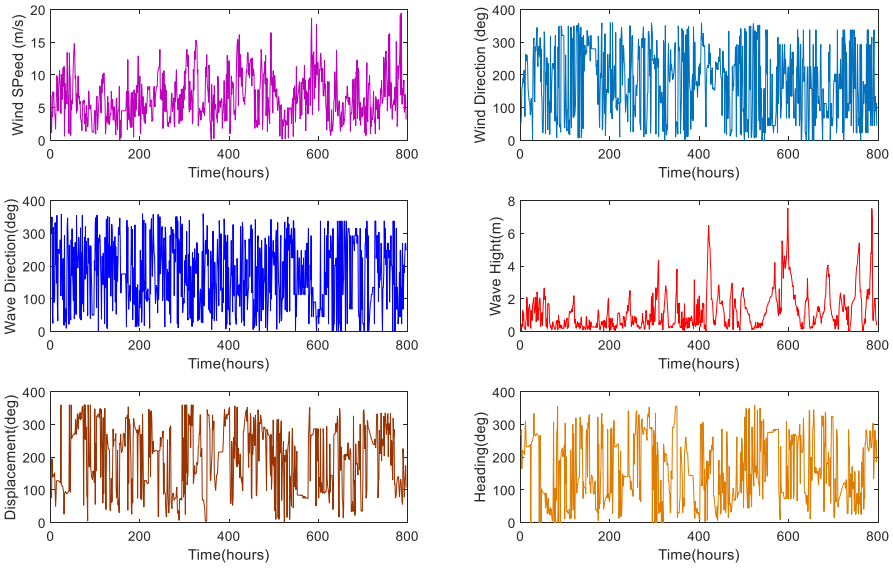

Figure 3-7. Historical weather and sea parameters, and ship movement for a month of operation [38].

As a result, an accurate input parameter improves DP power prediction in sea disturbances with more precision. Moreover, in this study, historical data of the requested DP power from PMS has been used as the dynamic and nonlinear historical data sets to predict the hourly, daily, and weekly thruster's power consumption. Hence, The requested DP power dataset is studied, and the power profiles are classified on sea state. For this reason, an accurate variety of input parameters improve the forecast of DP demand at sea disturbances. Hence, to analyze thrusters consumption related to sea states, Table 3-2 illustrates the classified range of DP demand from PMS related to weather conditions.

Table 3-2. The requested DP power from PMS in various sea states [38].

Descriptions			DP demand (MW)
Sea Conditions	Wave (m)	Wind (m/s)	
Calm-Slight	[0–1.25]	[0–5]	[0–1]
Moderate	[1.5–3]	[5–10]	[1–3]
Rough	[3.25–5.5]	[10–15]	[3–5]
High	[5.5–9.5]	[15–20]	[5–7]

Corresponding to the data sets collected shown in Figure 3-7 and Table 3-2, a non-linear correlation between the hourly DP load profiles and sea conditions such as

wave and wind is observed. Consequently, the effect of sea disturbances on the DP demand is shown in Figures 3-8 and 3-9. Therefore, the hourly changes of wave and wind and ship movement parameters are used as external inputs (disorders) in (3-13) and (3-14) to increase the accuracy of the learning procedure and speed convergence of the NARX based on LM-BP for DP load prediction.

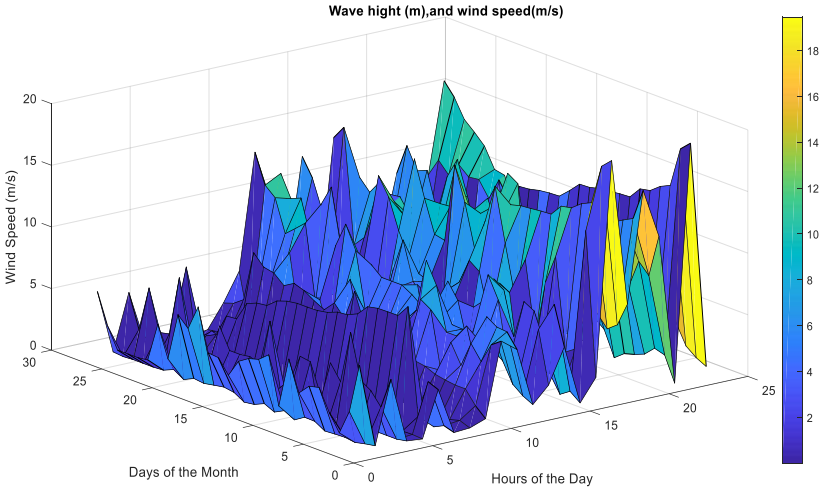

Figure 3-8. Relationship between wave height and wind speed in the sea disturbances [38].

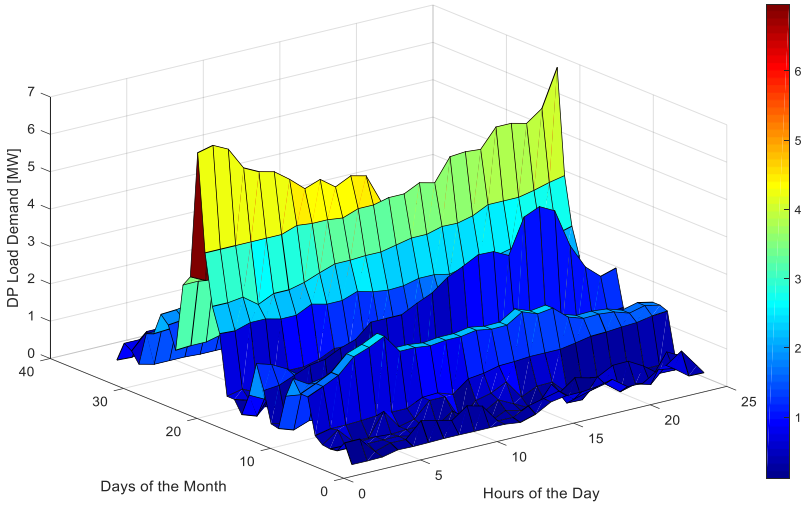

Figure 3-9. DP demand co-relationship with sea disturbances [38].

To validate and train the NARX as the proposed method, the equation (3-13) in section 3.2.2 is used to forecast one day lead DP power demand, where the actual DP power demand y(n,t) is defined at the time t and day n. Furthermore, according to the equation (3-14), $\hat{y}(n,t)$ is the NARX network output at time t and day n as the anticipated DP power where the adjusted weight vector w (n,t) and the NAF sigmoid $f(u)$ are defined in the mathematical relation. Table 3-2 illustrates the sea disturbances related to Figure 3-7. The $H(n,t)$, $W_{V2}(n,t)$, $W_{D4}(n,t)$, $W_{S3}(n,t)$, $D(n,t)$, and $W_{h1}(n,t)$ are specified as exterior inputs of $x(n,t)$ at the time t and day n in (3-13) and (3-14) correspondingly. Delay Lines T_{dy} and T_{dx} values are used as inputs of the NARX network to train the weights vector based on the LM-BP algorithm, as shown in Figure 3-10 [38].

Furthermore, for training and validating inputs and outputs, a toolbox related to deep learning in MATLAB is used to create the NARX network and compare it with other NN time series techniques such as NAR and TDL [62]. The percentage of the external inputs for training, validating, and testing is adjusted as 70%, 15%, and 15% correspondingly. In the next step, the neurons of the hidden layer are defined to 25 numbers. In conclusion, to predict hourly, daily, and weekly DP power demand, time delay *Tdy* and *Tdx* are determined for hourly forecasting from 1 to 24, daily 24 to 72, and weekly 168. Furthermore, the training procedure is executed offline to forecast the thruster's power consumption. The learning process's performance is analyzed to validate and test the trained parameters related to thrusters' actual power consumption. The hourly STLP regression plots of the trained, validated, and tested data sets epochs have been reasonably successful as shown in Figures 3-11 and 3-12, where the training, validation, and test of the data sets approximately 99 and 98 percent at mean square error (MSE) 0.033 at epoch 7 for 13 iterations respectively. Moreover, the regression of the figures is defined similarly for each single learning process.

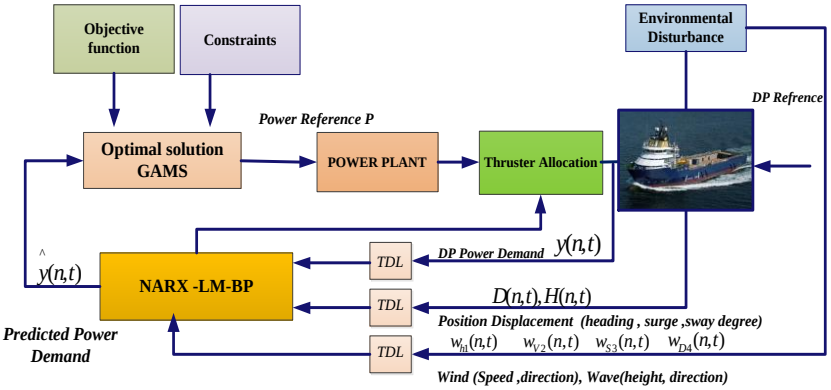

Figure 3-10. The NARX-LM-BP learning method in sea disturbances [38].

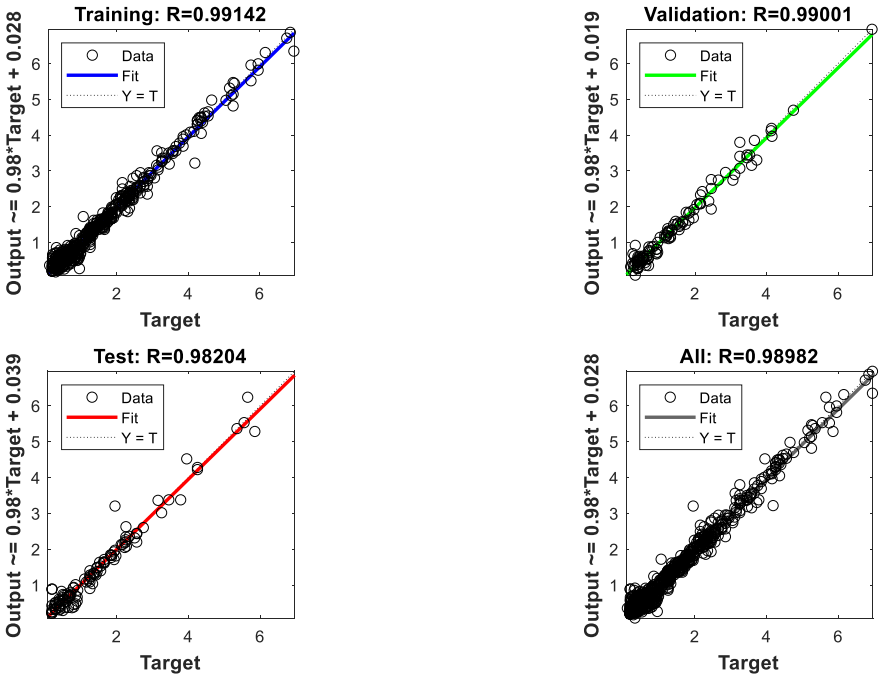

Figure 3-11. Regression model of the LM-BP-NARX [38].

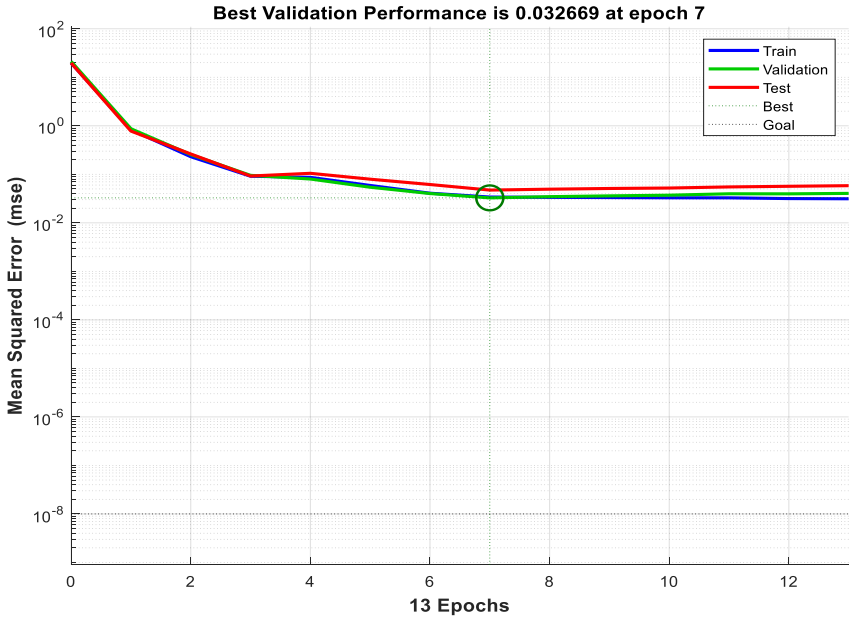

Figure 3-12. Performance of mean square error (MSE)

Most of the training set's extensive data generate the output results at the first-order line of the edge related to the best connection. Therefore, the correlation between real and anticipated power demand based on the NARX method presented in the target fitting line reveals that it can perform relatively well in the different sea conditions. In this study, the LM-NARX is evaluated with other NN based time series structures such as NAR, TDL via measurement indicators (MI). The error variance (δ_{er}) and the mean absolute percentage error (MAPE) is defined in [38]:

$$\delta_{er} = \sqrt{\frac{1}{N}\sum_{i=1}^{N}[y(n,t) - \hat{y}(n,t)]^2} \tag{3-15}$$

$$MAPE = \frac{1}{N}\sum_{i=1}^{N}\frac{\left|y(n,t) - \hat{y}(n,t)\right|}{y(n,t)} \times 100 \tag{3-16}$$

3.2.4. Results

As a result, to evaluate the NARX method performance, three scenarios are proposed. Scenario A is considered the actual and forecasted DP power consumption in various sea conditions for a month of DP operation. Scenario B weekly thrusters power consumption is analyzed the average error percentage of prediction. Scenario C is assessed the hourly load forecasting with the peaks of thrusters power consumption and percentage error from rough to calm sea condition at the multiples of 24-h lags. Finally, the NARX performance results in different scenarios are evaluated with the other time series categories.

3.2.4.1. Scenario A: DP power demand in sea disturbances

Sea disturbances influence the DP power demand from PMS for various hours and days of a month from calm -slight to rough and high conditions as shown in Figures (3-8) and (3-9), where the total peaks of thrusters power consumption in the diagram pattern occur between wild to high sea disturbances. Therefore to estimate power demand precisely, the effective disturbances pattern is defined as the external input for training the NARX network, which the other time serious schemes have not this possibility during the learning process. Hence, the comparison of the proposed method with other NN-time series schemes for a month of DP operation is shown in Figure 3-13 as a critical specific DP power demand that provides an hourly autocorrelation function of predicted power demand.

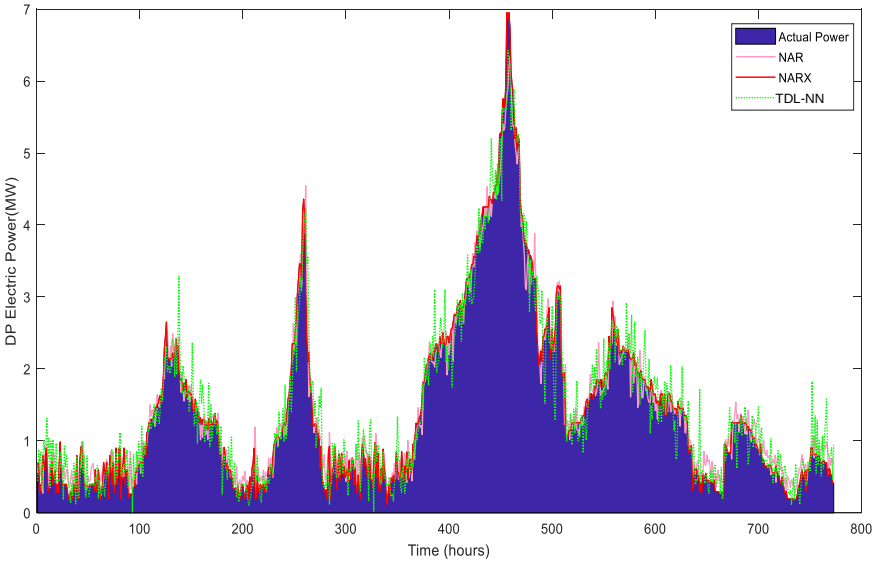

Figure 3-13. The STLP comparison for a month of DP operation [38].

The power consumption reasonably is lower in the calm-slight state than in the moderate situation. The results have been achieved based on MI performance as defined in equations (3-15) and (3-16) for 31 days of STLP in different sea conditions, where they have been categorized as inputs into the NARX model in Table 3-2. The comparison average error values of the δ_{er} and MAPE for predicting the requested DP power based on the NARX method with the NAR and TDL are shown in Figures (3-14) and (3-15) around 0.13 MW and 0.08%, respectively. The maximum error percentage of the requested DP power from PMS based on STLP is related to the TDL method nearby to 0.2 MW and 0.12%.

Furthermore, the NAR method is performed more precisely compare with the TDL-NN, where the MAPE and δ_{er} error in Table 3-3 are defined around 0.11% and 0.17 MW. Nevertheless, due to the absence of sea distortion parameters as external inputs in NAR and TDL-NN during the offline network learning, the NARX method is more accurate than the other time series NN scheme.

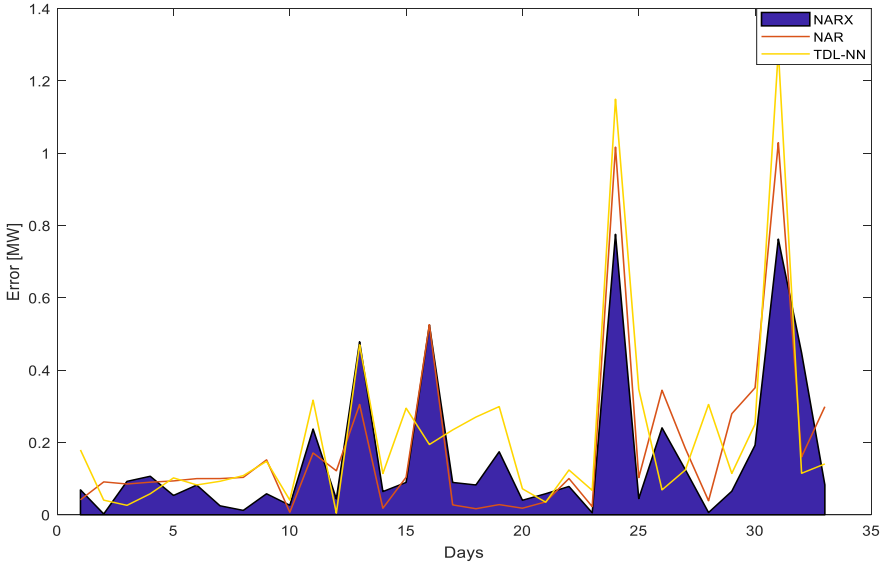

Figure 3-14. The error variance δ_{er} of STLP for a month of operation [38].

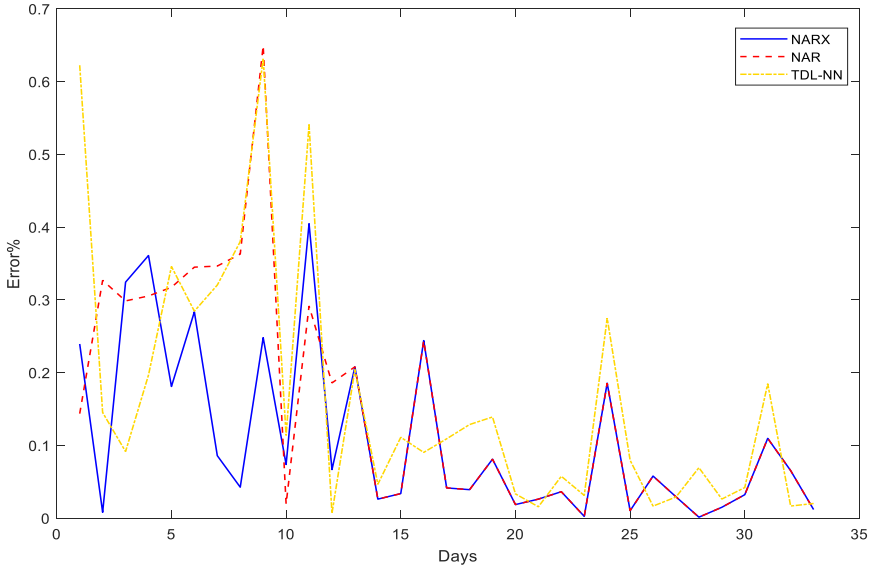

Figure 3-15. The error percentage of MAPE for the STLP in a month [38].

Table 3-3. Comparison of predicted DP power demand in a month of operation [38].

Sea States	NAR-NN		NARX-NN		TDL-NN	
	δ_{er} (MW)	MAPE (er) (%)	δ_{er} (MW)	MAPE (er) (%)	δ_{er} (MW)	MAPE (er) (%)
Calm sea	0.1	0.3	0.07	0.11	0.1	0.3
Moderate sea	0.11	0.08	0.1	0.07	0.18	0.08
Rough sea	0.33	0.07	0.2	0.05	0.35	0.08
Extrem rough sea	0.15	0.02	0.12	0.018	0.15	0.02
Average	0.17	0.11	0.13	0.08	0.2	0.12

3.2.4.2. Scenario B: Weekly DP power demand in different sea states

In Scenario B, to forecast weekly load demand, the previous seven days with delayed of 7 × 24-h (168 h) and the past three days of sea distortion with delayed 24, 48, and 72 of DP operation is applied in equations (3-13) and (3-14) as practical inputs during the NARX training method. The total number of inputs according to Table 3-1 and neurons in hidden layers is regulated 7 and 25 correspondingly. While the NARX model learning process is implemented, it can predict the 24-hours power demand using the 24 hours weather forecast and motion sensors parameters, as shown in Tables 3-1 and 3-2. In Table 3-4, the average weekly DP power demand is analyzed, which changes in different sea conditions among the days of weeks in a month.

A strong relation is observed in thrusters power consumption on weekdays, where the power demand due to calm-slight sea conditions is less than the rough and high sea states. Therefore, the comparison average error values of the δ_{er} and MAPE for predicting the requested DP power based on the NARX method with the NAR and TDL are shown in Figures (3-16) and (3-17), approximately 0.12 MW and 0.12%. At the same time, the maximum error percentage of STLP for the DP demand is related to TDL nearby 0.19 MW and 0.18%, correspondingly. Moreover, the NAR network process is executed more precisely compare with the TDL as presented in Tables 3-4 by δ_{er} error 0.16 MW and MAPE of 0.17%. Nevertheless, due to the absence of sea distortion parameters as external inputs in NAR and TDL during the offline network learning, the NARX method is more accurate than the other time series NN scheme.

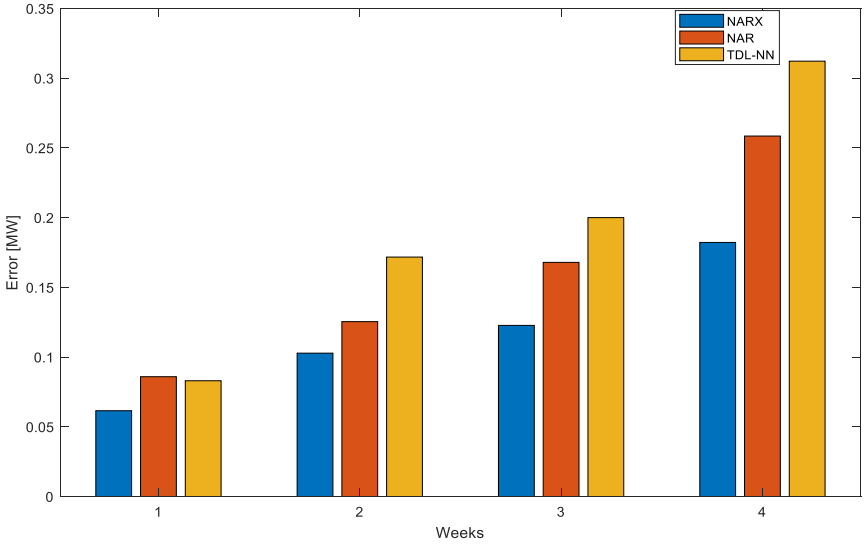

Figure 3-16. The error variance (δ) for weekly STLP in a month of DP operation [38].

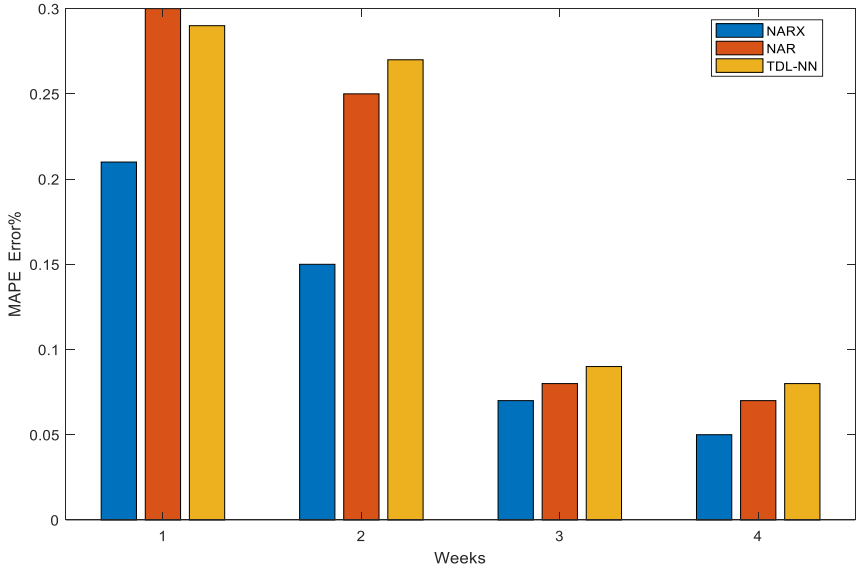

Figure 3-17. The error percentage of (*MAPE*) for the weekly STLP in a month [38].

Table 3-4. Comparison of weekly DP demand predicting in different sea states [38].

Week	NARX-NN		NAR-NN		TDL-NN	
	δ_{er} (MW)	MAPE*er* (%)	δ_{er} (MW)	MAPE*er* (%)	δ_{er} (MW)	MAPE*er* (%)
1st	0.06	0.21	0.09	0.30	0.08	0.29
2st	0.10	0.15	0.13	0.25	0.17	0.27
3st	0.12	0.07	0.17	0.08	0.20	0.09
4st	0.18	0.05	0.26	0.07	0.31	0.08
Average	0.12	0.12	0.16	0.17	0.19	0.18

3.2.4.3. Scenario C: Hourly DP power demand in different sea states

Finally, the NARX network can predict the hourly power consumption of thrusters for PMS to economically dispatch between DGs and ESS in sea disturbances. The requested DP power from PMS is classified into sea state patterns and hours in a DP operation. The matrix of weights vector is estimated at time intervals *t* and first day via using the earlier requested power dataset for each load sample in the equations (3-12), (3-13), and (3-14). Accordingly, the time delay *Tdx* and *Tdy* values are defined in [38] as time intervals $x_1(1,t-1),...,x_6(1,t-2), y_1(1,t-1), y_1(1,t-2)$ in the equation (3-14) to train the NARX network for hourly DP prediction based on sea disturbances (total seven inputs). Consequently, the average error values of the δ_{er} and the MAPE for predicting the requested DP power based on NARX and time series NN methods such as NAR and TDL-NN are compared in Figures (3-18) and (3-19). The hourly details of DP power demand prediction results in the MI performance are analyzed in Table 3-5. Accordingly, the maximum error percentage of STLP for thrusters power consumption is related to TDL-NN approximately 0.49 MW and 0.75%, respectively. Furthermore, compared with TDL-NN performance, the NAR network's MAPE and δ_{er} error are predicted more precisely around 0.43 MW and 0.65%, as presented in Table 3-5. As a result, MI's minimum performance percentage error belongs to the NARX method for forecasting 1 to 24 h lead thruster power demand by δ_{er} error 0.12 MW and MAPE of 0.18%. Hence, the proposed method is presented with high accuracy, reliability, and minimum error percentage to predict hourly DP demand compare with another NN-time series scheme [38]. Furthermore, the speed convergence of the training run-time of NARX with the other NN-time series is investigated in three scenarios to ensure that the proposed method's speed of learning processes has high performance. As a result, the NARX learning process is about 5.2 seconds, less than the TDL-NN and NAR network, with a run time of around 6.65 seconds and 208.5 seconds in scenario C, correspondingly. Similarly, results for other scenarios A and B can be observed in Table 3-6 [38].

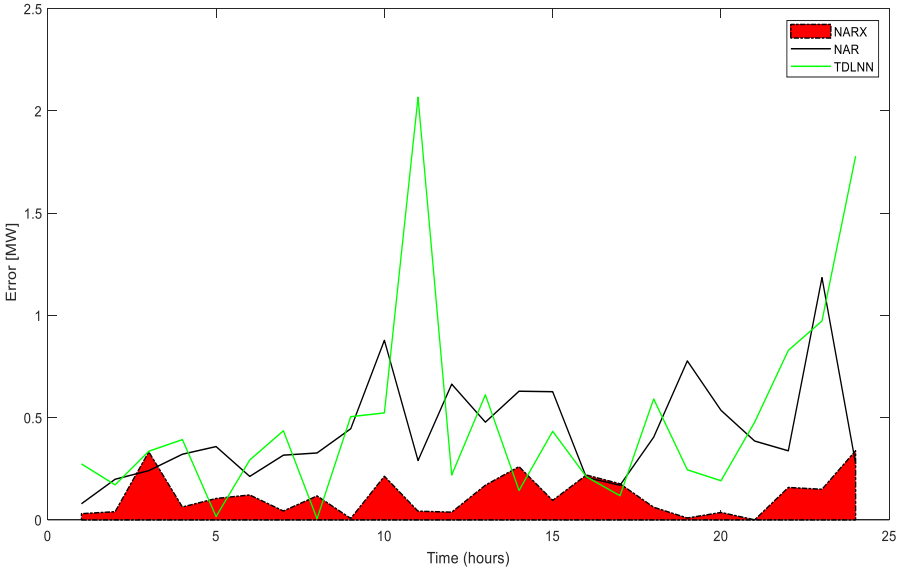

Figure 3-18. The error variance (δ) for hourly STLP of DP operation [38].

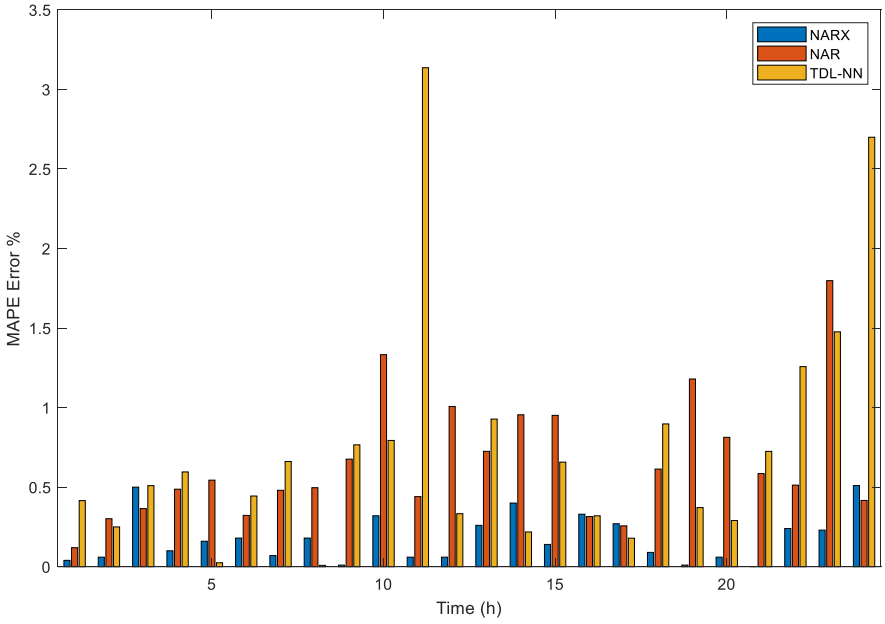

Figure 3-19. The error percentage of (*MAPE*) for hourly STLP[38]

Table 3-5. Comparison of hourly DP demand prediction in different sea states[38]

Hours	NARX-NN		NAR-NN		TDL-NN	
	δ_{er} (MW)	MAPE*er* (%)	δ_{er} (MW)	MAPE*er* (%)	δ_{er} (MW)	MAPE*er* (%)
1	0.03	0.04	0.08	0.12	0.27	0.42
2	0.04	0.06	0.20	0.30	0.17	0.25
3	0.33	0.50	0.24	0.37	0.34	0.51
4	0.06	0.10	0.32	0.49	0.39	0.60
5	0.10	0.16	0.36	0.54	0.02	0.02
6	0.12	0.18	0.21	0.32	0.29	0.44
7	0.04	0.07	0.32	0.48	0.44	0.66
8	0.12	0.18	0.33	0.50	0.01	0.01
9	0.01	0.01	0.45	0.68	0.50	0.77
10	0.21	0.32	0.88	1.33	0.52	0.79
11	0.04	0.06	0.29	0.44	2.07	3.14
12	0.04	0.06	0.66	1.01	0.22	0.33
13	0.17	0.26	0.48	0.73	0.61	0.93
14	0.26	0.40	0.63	0.95	0.14	0.22
15	0.10	0.14	0.63	0.95	0.43	0.66
16	0.22	0.33	0.21	0.32	0.21	0.32
17	0.18	0.27	0.17	0.26	0.12	0.18
18	0.06	0.09	0.40	0.61	0.59	0.90
19	0.01	0.01	0.78	1.18	0.24	0.37
20	0.04	0.06	0.54	0.81	0.19	0.29
21	0.00	0.00	0.39	0.59	0.48	0.72
22	0.16	0.24	0.34	0.51	0.83	1.26
23	0.15	0.23	1.18	1.80	0.97	1.48
24	0.34	0.51	0.27	0.42	1.78	2.70
Average	0.12	0.18	0.43	0.65	0.49	0.75

Table 3-6. Training run-times in different scenarios methods[38]

Training time / Scenarios No.	NARX-NN	NAR-NN	TDL-NN
Scenario A	1.069	1.556	3.154
Scenario B	1.760	1.839	38.902
Scenario C	5.223	6.652	208.526

CHAPTER 4. POWER MANAGEMENT SYSTEM

This chapter discusses the widespread use of the DP ship's power system, which the papers have been published in [11], [38], and [13]. This section also includes contributions of ESS to decrease GHG emissions and pick shavings. The proposed optimization method utilizes an interactive approach based on the GAMS and machine learning method to improve its computational performance. The proposed NARX method in Chapter 3 predicts DP power demand for PMS to minimize operating costs, limiting GHG emissions, and providing technical and operational constraints based on the GAMS algorithm.

4.1 Methodology

The motivation for investigating progressive power management technologies have been developed efficiently and greener for all existing energy subsystems [2] and[5]. In this regard, due to its direct impact on increasing the efficiency of ships, an optimal energy management strategy has been used to obtain efficient operation from each power unit by economic dispatching to solve optimization problems [11],[6]. In a DP ship, power system reliability is crucial due to DP operation, which is equipped with propulsion systems and variable frequency drive (VFD) for the drilling system to operate successfully. Nevertheless, one of the most efficient solutions to ensure power quality and reliability is ESS for the DP shipboard system with the greater penetration of other distributed generations [5]. Furthermore, an ESS can significantly manage the DP and other dynamic demand and global DP ship power management in general by reducing the potential of main engines, which decreases operating costs [63],[64]. For instance, in [65], [66], [67], and [68], a lithium-ion battery ESS is assigned for hybrid power plants including diesel engines, ship hotels, and service load consumption to minimize fuel consumption and spinning reserve.

Another factor that has not been utilized sufficiently in DP ships, using ESS can significantly minimize operational cost, spinning reserve, fuel cost, and GHG emissions [7],[71]. The DP shipboard power system's target is to optimize the power generation and ESS by optimally adjusting ship motion and power generation with the possible economical cost using the optimal DGs operation point. These performance goals are subject to different technical solutions and operational constraints such as power balance, generators' ramp rates, generators' loading, minimizing up and downtimes, ship motion limitation, etc. It should be remarked that

the DP demand management and optimal power generation problems are respectively joined. Furthermore, the problem under study requires complex methods to solve the optimization problem that can meet the above challenges. In [11], an optimal solution is proposed using the particular swarm optimization (PSO) technique for a DP drillship to solve economic dispatch by considering six operational diesel generators with ramp rate limits. The proposed method shows high performance due to DGs' nonlinear features, such as non-smooth cost and generators ramp rate constraints in the drilling and DP operation. The PSO method is used to solve the DP ships' optimization and economic dispatch problem during the drilling operation [11]. However, by applying battery ESS and predicted power demand in different weather sea states, the PSO method was not reliable due to the low speed of convergence for large scale of the time intervals and non-smooth diesel generators cost function.

In this thesis, an efficient optimization model is performed for optimal economic dispatch with five diesel generators in the presence of a battery ESS (BESS) unit for a typical DP drill ship's power plant system. Hence, the model is expressed as a multi-objective boundary decision making with mixed-integer nonlinear programming (MINLP) optimization problems. The multi-objective function is also determined to minimize the sum of operational, emissions, and fuel costs appropriately annualized. Moreover, It Should be mentioned that the simulation and MINLP algorithms are performed in the GAMS as an advanced modeling system designed for solving optimization problems such as MINLP, non-linear (NLP), and linear programming (LP) as the main engine of optimization [70]. Furthermore, the baron solvers are used to enable the users to connect the capabilities of GAMS as high-level modeling software for solving objective functions with the ability of optimizers. As a result, the proposed optimization algorithm is executed in the GAMS modeling software. A typical DP drillship is selected for economically dispatching between DGs and BESS during the DP and drilling operations. The summary of the shipboard power system's technical specifications, power plant, and BESS is presented in Table 4-1 and Table 4-2. The DP ship power plant is designed for five DGs of 3600KVA with nominal active power connected to propulsion load, drilling system, and hotel load by AC/DC and DC/AC converters.

Furthermore, two three-phase transformers for service, hotel load, and two transformers using the 3600 KVA as nominal power for drilling and DP operation propose several feeders and circuit breakers. Figure 4-1 expresses the schematic diagram of a typical DP drillship power generation and distribution system. In this simulation, DG power operates on generator limitations such as ramp rates, fuel, and emission cost-performance coefficients, as shown in Table 4-1[11].

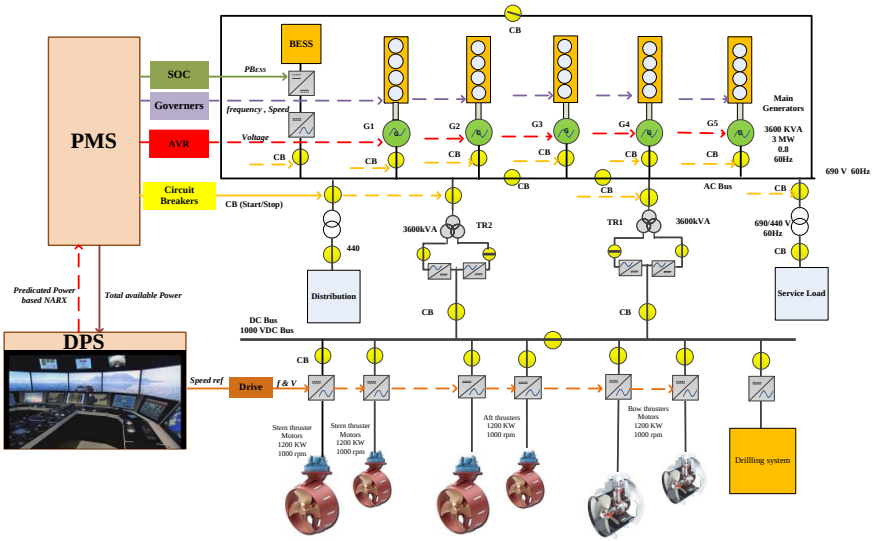

Figure 4-1. The schematic relationship diagram between the PMS and DPS[11].

Table 4-1. Generators' capacity and coefficients used for DP ship[11].

Unit No.	$P_i^{\min}$ (MW)	$P_i^{\max}$ (MW)	θ ($)	β ($/MW)	γ ($/MW^2)	URi (MW/h)	DRi (MW/h)
g1	*0.75*	*3*	*230*	*7*	*0.007*	*0.8*	*0.8*
g2	*0.75*	*3*	*230*	*10*	*0.0095*	*0.8*	*0.8*
g3	*0.75*	*3*	*230*	*8.5*	*0.009*	*0.8*	*0.8*
g4	*0.75*	*3*	*230*	*11*	*0.009*	*0.8*	*0.8*
g5	*0.75*	*3*	*230*	*10.5*	*0.008*	*0.8*	*0.8*

Table 4-2. Battery capacity and coefficients used for DP ship

Parameter	Description	Value
$P_L(t)$	*Total load energy demand,*	*5903.54 MWh*
P_{Sfoc}^{Opt}	*Fixed speed gen-sets optimal loading,*	*30-90%*
$Ess_{Bat}^{\max}$	*Maximum battery capacity*	*1.2 MWh (100%)*
$Ess_{Bat}^{\min}$	*Minimum battery capacity*	*200 KWh (20%)*
$P_{Bdis}^{\max}$ & $P_{Bcha}^{\max}$	*Maximum discharge and charging rate*	*900 kW*
$P_{Bcha}^{\min}$	*Minimum battery charging rate*	*0 kW*
η_{Bcha}	*Battery charging efficiency*	*95%*
η_{Bdcha}	*Battery discharging efficiency*	*90%*
$SOC_{B\min}$	*Minimum battery sate of charging*	*20%*
$SOC_{B\max}$	*Maximum battery sate of charging*	*100%*

4.2. Problem descriptions

The problem definition is to identify the optimal operational planning and economic dispatch of MINLP optimization for the DP drillship power plant systems. Exclusively, for drilling and DP operation that has a higher priority to other consumers where the power demand in heavy operation condition imposed power limitation of generators. Therefore, the proposed hybrid power unit for each particular time of DP operation period must be estimated by the NARX model for PMS/EMS to dispatch economically between power plants. An optimal operation for power units is proposed for power demand for the DP system to maximize energy efficiency by using spinning reserve and generators limitation and BESS, which are contained ramp rate limits and state of charging (SOC) boundary respectively.

4.2.1 Shipboard generators operation limitations

In the shipboard system, to solve the problem of economic dispatch for DP drillship generation units, it is assumed that generators' output is regulated immediately and efficiently. Practically, all DG units' operation range is bounded via their ramp rates to regularly limit the generation units' operation range. Hence, limitations of DGs setup are taken between the lower ramp (LR_i) and upper ramp rate (UR_i) boundaries of generators settings as follows [11]:

$$P_{i,t}^{dg} - P_{i,t-1}^{dg} \le LR_i \tag{4-1}$$

$$P_{i,t-1}^{dg} - P_{i,t}^{dg} \le UR_i \tag{4-2}$$

$$P_i^{dg,\min} \le P_i^{dg} \le P_i^{dg,\max} \tag{4-3}$$

where the $P_{i,t}^{dg}$ expresses output power, and the $P_{i,t-1}^{dg}$ previous output power of i_{th} the generators.

4.2.2 Generators and battery operation constraints

The optimization problem cost function of *Ob* is solved by considering the power balance, BESS, and generator limitations at the specific operational at time intervals, which can be represented as [11],[6]:

$$\sum_{i=1}^{m} P_{DG,i} + P_{Bdisch} = P_L + P_{Bcharge}, i = l,...,m. \tag{4-4}$$

$$\max(P_{i,t}^{dg,\min}, P_{i,t}^{dg} - LR_i) \le P_{i,t}^{dg} \le \min(P_{i,t}^{dg,\max}, P_{i,t}^{dg} + UR_i) \tag{4-5}$$

where the P_L is the total demand included DP and drilling load profiles at operational

time intervals. Moreover, the P_B is the active power of the battery and characterized by the maximum and minimum power rate in both discharging and charging stages, which the P_{Bch} and P_{Bdis} rates cannot be exceeded as the following equations [6]:

$$0 < P_{Bdis} < P_{Bdismax} \tag{4-6}$$

$$0 < P_{Bch} < P_{Bchmax} \tag{4-7}$$

The state of battery charging SOC_B at the time interval *t* is defined as maximum $SOC_{B\max}$ and minimum $SOC_{B\min}$ values as following boundaries [7]:

$$SOC_{B\min}(t) < SOC_B(t) < SOC_{B\max}(t) \tag{4-8}$$

$$SOC_B(t) = SOC_B\left(t-1\right) - \eta_B(t) \times P_{Bcha}(t) \times \Delta t \tag{4-9}$$

$$\eta_B(t) = \begin{cases} \eta_{Bcha}(t) & if \quad P_B(t) < 0 \\ \dfrac{1}{\eta_{Bdis}(t)} & if \quad P_B(t) \geq 0 \end{cases} \tag{4-10}$$

where the η_{Bdis} and η_{Bcha} are the discharging and charging efficiency, respectively. The SOC_B efficiency in (4-9) depends on the battery's energy level, charging, and discharging at time intervals. The minimum and maximum values of the SOC_B in (4-8) are specified in the maximum permissible depth of BESS discharging as an estimated lifetime. According to PMS/EMS strategy, the battery SOC_B must be fully charged initially to compensate for the *DP* demand during the drilling operation.

4.2.3 Specific fuel oil consumption

In the presence of DP demand in the shipboard system, DGs operate under different operational conditions. Accordingly, the engines are not operated under the optimal loading conditions, in which the fuel consumption increases in different engine loading percentages [7]. Specific fuel oil consumption (SFOC) measures DGs' fuel efficiency and engine performance in loading percentage, producing power by consuming fuel [71]. The DGs' operation in optimal points is analyzed based on the SFOC curve to improving engine performance and fuel consumption. Typically, the

optimal loading for the DGs scale is between 60 and 90% of the measured engine power. The engine operation in this range significantly reduces SFOC to minimum rates and maximum operational efficiency based on shop trial [71] as defined in Figure 4-2. Hence, the SFOC is applied to measure the fuel consumption of shipboard engines. In this regard, there are various methods for estimating marine engines' fuel consumption to identify the quality of SFOC and GHG emissions factors that are crucial to assessing the fuel oil consumption and harmful gas emissions, respectively [71].

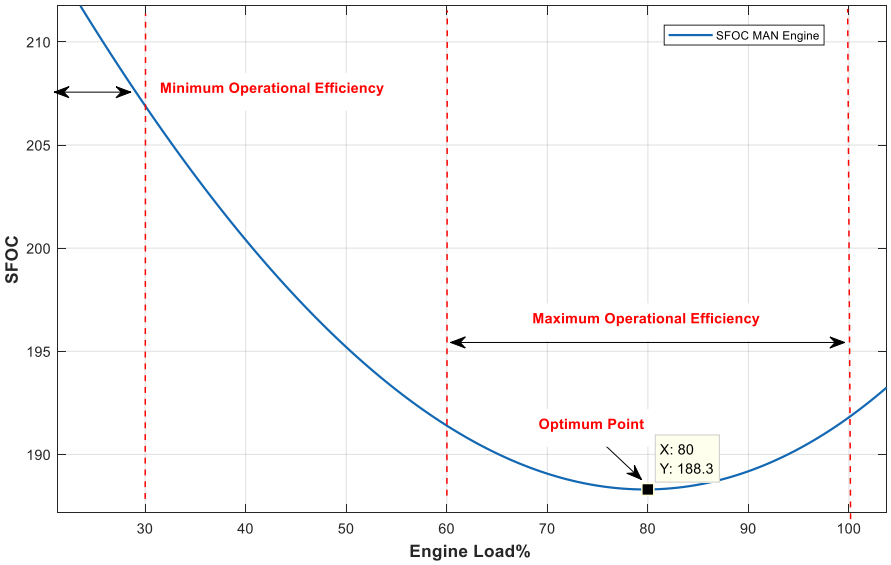

Figure 4-2. The SFOC curve is based on the fixed speed gen-set operation

According to [7], it can be represented as a quadratic function by third-degree polynomial function between actual at $P_{Dgt,j}$ and the rated power P_n of the DGs via curve fitting of engine loaded percentage values:

$$Sfoc_{t,j} = a\left(\frac{P_{Dg_{t,j}}}{P_n}\right)^3 + b\left(\frac{P_{Dg_{t,j}}}{P_n}\right)^2 + c\left(\frac{P_{Dg_{t,j}}}{P_n}\right) + d \quad t = 1,...,n \quad j = 1,...,m \left[\frac{g}{kwh}\right] \tag{4-11}$$

where a i_{th}, b i_{th}, c i_{th} and d are the coefficients of fuel emission of the i_{th} power units used in (4-11) as: $a = -0.22$, $b = 1.1$, $c = -1.2$, $d = 232$. The fuel consumption

is defined by utilizing the power flow in the equations of (4-11) depends on the SFOC reference. Therefore, another crucial *Ob* function corresponded to the SFOC for minimizing the DGs fuel consumption (FC) is displayed in the discrete-time area as presented in [7]:

$$Total\ \ fuel\ consumption = \sum_{t=1}^{m}\sum_{j=1}^{n}(Sfoc_{t,j}.P_{Dg_{t,j}}\Delta t)\ \ t=1,...,n\ \ \ j=1,...,m\left[\frac{g}{h}\right] \tag{4-12}$$

where *n* is the number of *DGs* in the *DP* operation at *Sfocn* corresponds to the power delivered by all DGs in *kW*, and *t* is the time intervals between samples, and the sub-index *m* is the number of the selection. Moreover, reducing DG emissions is a significant factor that several frameworks are introduced to estimate and calculate marine ships' emissions [9]. For this proposed, fuel consumption is essential to evaluate the emission rate during the DP operation. Hence, to solve the optimization problem using the proposed method, DGs' emission coefficients are considered in equation (4-12). Furthermore, to analyze the estimated carbon dioxide (CO2), sulfur oxides (SOX), and nitrogen oxides (NOX) emissions, as maximum emissions from the vessels, the equations (4-13) to (4-15) can be estimated as following [71]:

$$NO_X = emf_{NO_X}\sum_{t=1}^{m}\sum_{j=1}^{n}P_{Dg_{t,j}}\quad j=1,...,m\qquad [g] \tag{4-13}$$

The NOx emission factor emf_{NO_X} is based on generated power to each engine given in g/kWh, and the total NOx mass is released in [g]. The amount of SOX and CO2 emission factors emf_{SO_X} and emf_{CO_2} are specified in [kg] per 1000kg of consumed fuel factors, so it depends on the mass of the fuel consumption. Depending on the amount of SOX emissions, the fuel's sulfur content is considered in the equation of (4-14) [71].

$$SO_X = emf_{SO_X}\sum_{t=1}^{m}\sum_{j=1}^{n}(Sfoc_{t,j}.P_{Dg_{t,j}})\ \ t=1,...,n\ \ j=1,...,m\quad [kg] \tag{4-14}$$

$$emf_{SO_X} = 20\times\%\ sulfur\ \ mass$$

Furthermore, the mass of CO2 emitted into the environment is defined as the following equation [71]:

$$CO_2 = emf_{CO_2}\sum_{t=1}^{m}\sum_{j=1}^{n}(Sfoc_{t,j}.P_{Dg_{t,j}})\ \ t=1,...,n\ \ j=1,...,m\quad [kg] \tag{4-15}$$

By taking the above equations from (4-13) to (4-15) into the proposed method for solving the optimization problem and reducing fuel consumption and GHG emissions, results are presented in section 4.3. The reduction of fuel consumption and increasing

DG performance are obtained by running the engines at maximum load percentage, defined in Figure 4-2 and section 4.2.3 to estimate the SFOC to calculate the engine's fuel consumption.

4.2.4 Objective functions

In this project, the main purpose of economic dispatching is to decrease the operational rate cost during the DP and drilling operation of a DP shipboard system above different restrictions. The entire cost function of diesel generators specified by equation (4-15) as the quadratic curve fitting that in the table (4-1), the generators' coefficients are presented [11].

$$Op\cos t = \sum_{t=1}^{n}\sum_{i=1}^{m}\gamma_i P_{DG,i}^2 + \beta_i P_{DG,i} + \theta_i \qquad (4\text{-}16)$$

The environmental dispatching of electric power plants concerns environmental pollution. The environmental pollutions produced by DGs as thermal units depend on the type of marine diesel fuel (HFO, MGO), which they used to generate electricity for the shipboard system as expressed in the equations (4-11) and (4-12). Hence, to minimize the total fuel consumption (TFC) as the principal objective function in (4-12) and DGs operational cost function in (4-16), the optimization problem must be solved by multi-objective functions as:

$$MinOb = Op\cos t + TFC \qquad (4\text{-}17)$$

4.3. Results

In this study, three cases are executed to evaluate the predicted demand, including the DP and drilling operations in the different sea states. The forecasted DP demand has been discussed relatively in chapter 3 [38]. In these cases, the DP ship operating phases are examined with PMS/EMS strategy based on the STLP performance strategy to forecast the DP load patterns in different sea conditions, as described in section 3.2.4. The hourly predicted power demand is evaluated for PMS/EMS in environmental sea disturbances from calm to high and low to high DP operation in the presence of BESS. Concentrates on the hybrid AC/DC and DC/AC link, as shown in Figure 4-1, the BESS is equipped with the lithium NMC/LMO battery, and capacity of 1.2MWh, and the maximum depth of BESS discharging is assumed 90%.

The BESS is connected to the AC busbar via applying the bidirectional DC-DC, and DC/AC converter, where the BESS rated power is 900 KW. The dynamic loads

included the DP and drilling loads connected to DC link via DC/AC converter interface. The efficiency of converters in both AC and DC is defined as 98% of inverter and rectifier operation mode. Specifically, in the presence of dynamic loads linked to the DC busbar, the lowest rate of the AC/DC converter link voltage is imposed of 0.99 *pu*. In this case, when the PMS strategy is used to the shipboard power system with five generators in BESS's presence contrast to applying five generators without BESS, as shown in Figure 4-1.

An optimal PMS power reference is reduced fuel consumption and GHG emissions. Hence, the PMS produces suitable power references using BESS permission given to the DGs to operate at optimal values based on the SFOC curve expected from equation (4-11) related to the predicted load profile. Accordingly, the power references are optimized based on the multi-objective function (4-17) by considering DGs and BESS boundaries. An MINLP method is used in GAMS software to reduce fuel consumption and harmful emissions and peak shaving in BESS the optimum power setpoints.

4.3.1 Case study A: Economic dispatch of generators with BESS based on predicted DP power demand in sea state for a month of operation

The result of Case (a) is evaluated to investigate the proposed method performance in the presence of BESS in different sea conditions based on predicted power demand by the NARX network in section 3.2.4.1. As a result, Figure 4-3 shows an optimal strategy has applied by PMS to prevent the blackout in the peak load in the period of 400 to 500 hours due to high DP operation and compensates the oscillations of generators in the presence of BESS in Figure 4-4. Moreover, Figure 4-5 shows the hourly dispatch of BEES for different DP operations based on MINLP methods to produce optimal power generations between gen-sets.

Furthermore, it is observed that batteries charge DGs at their optimum operating point based on SFOC in Figure 4-2 and consume less fuel per unit of energy than conventional electric propulsion settings. Therefore, Figure 4-6 shows the optimal operation points in 188.3[g/kwh] and maximum efficiency of engine load percentage-based SFOC surface changes between 70 to100 percent. Meanwhile, in BESS's absences, the optimal solution is infeasible, and generators are produced non-optimal power references, as shown in Figure 4-7. Hence, generators are operated in low efficiency based on the SFOC surface and change between 25 to100 percent of engine rate as illustrated in Figure 4-8.

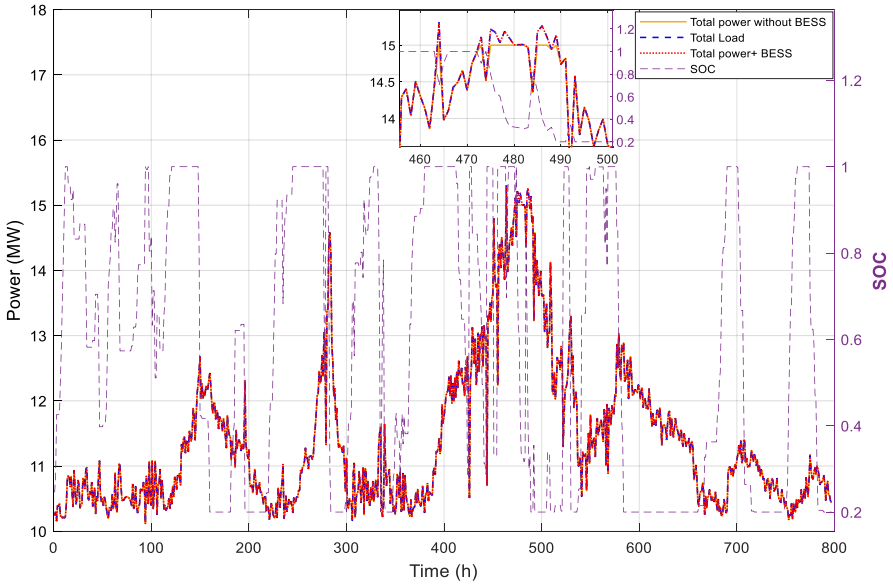

Figure 4-3. Optimal operation of DP ship for predicted power demand integrated with BESS.

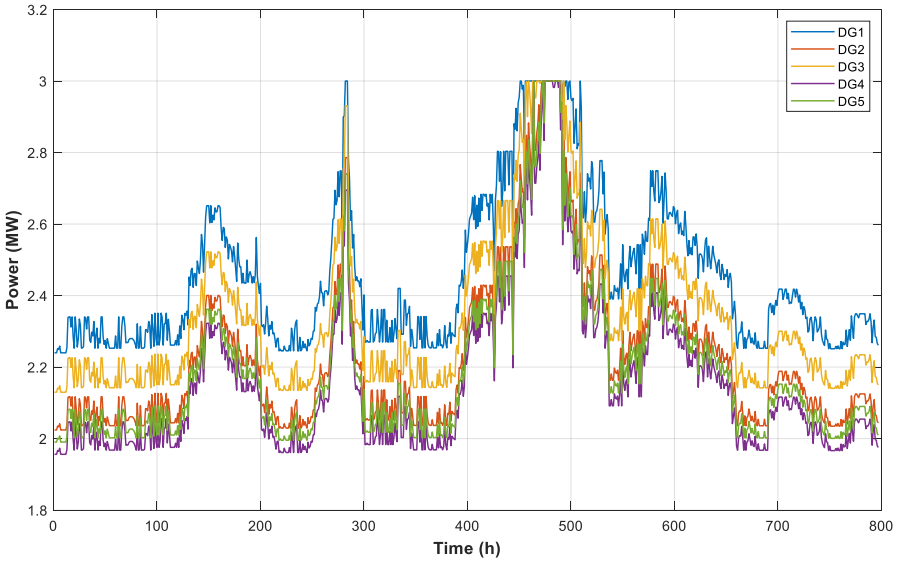

Figure 4-4. Optimal power generation of DGs based on BEES and MINLP methods.

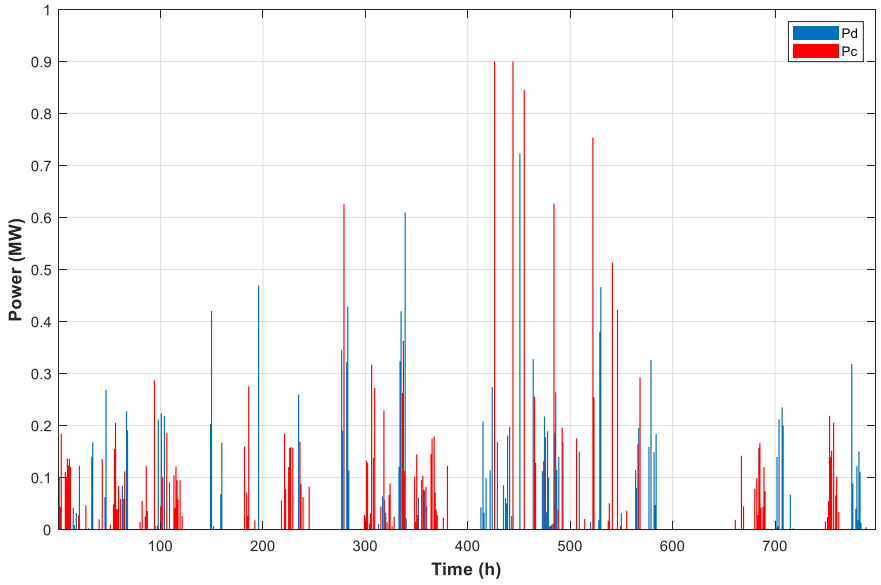

Figure 4-5. The hourly dispatch of BEES is based on MINLP methods for different DP operations.

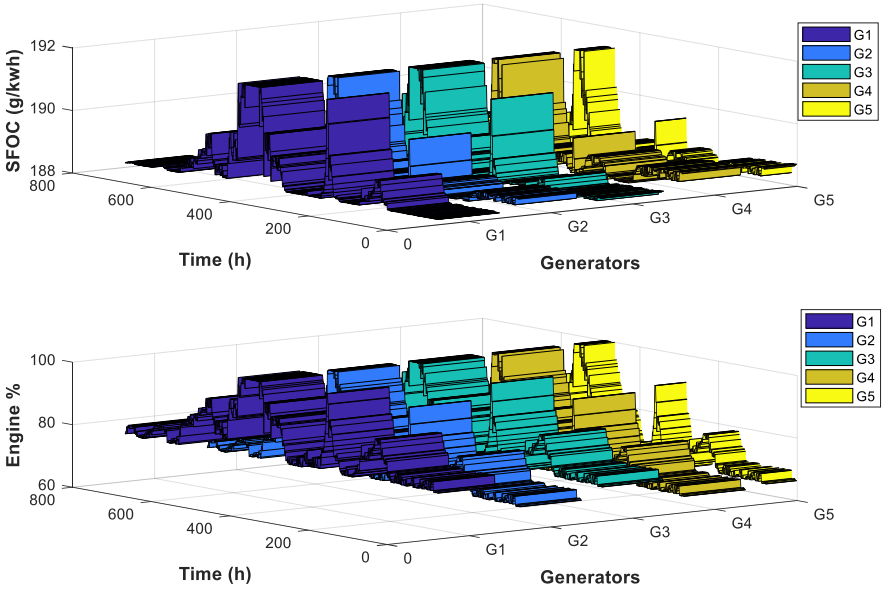

Figure 4-6. The SFOC curve is based on engine loading percentage for five gen-sets with BESS in a month of operation.

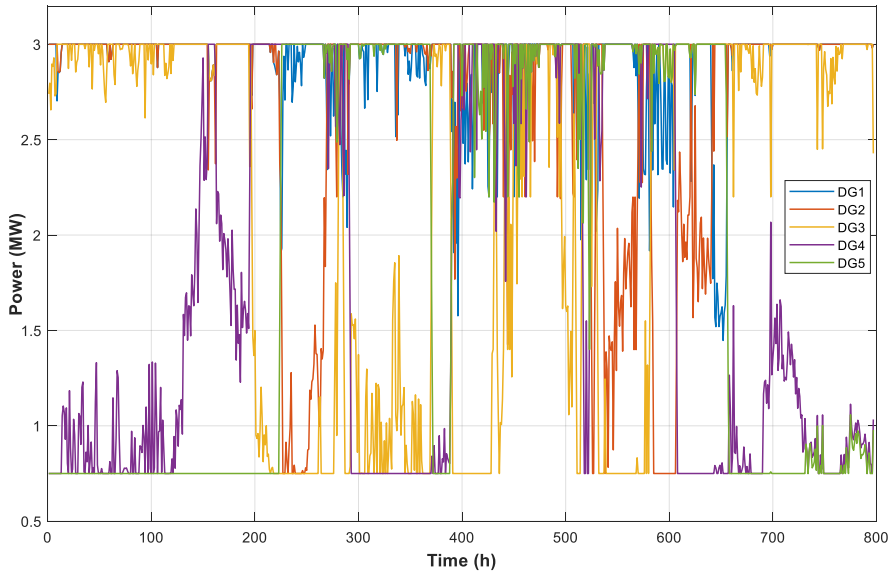

Figure 4-7. Hourly power generation of DGs without BESS and MINLP methods.

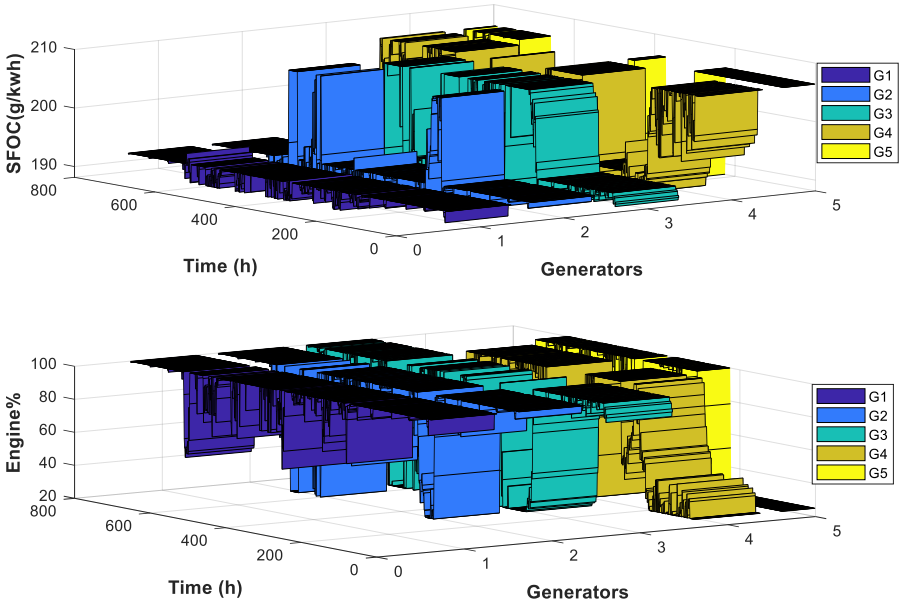

Figure 4-8. The SFOC curve is based on engine loading percentage for five gen-sets without BESS in a month of operation.

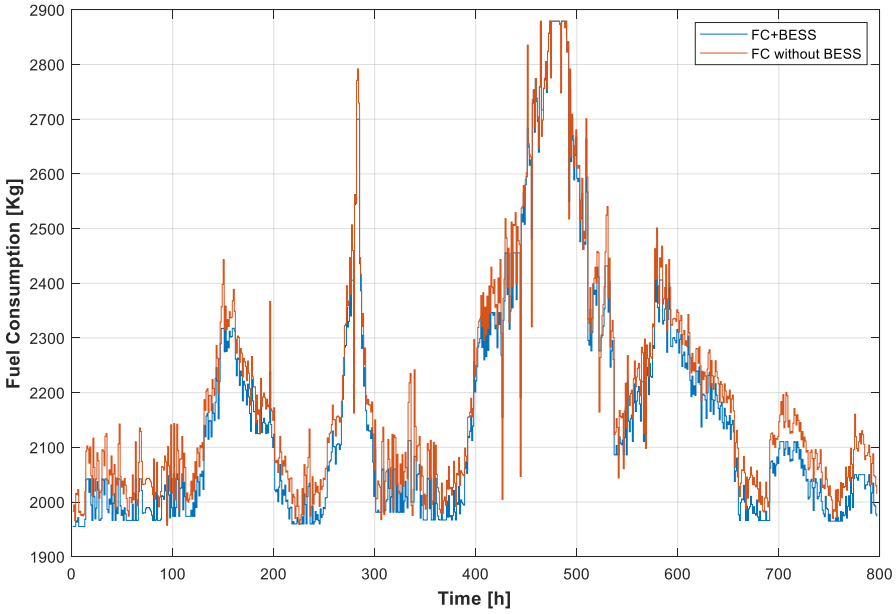

Figure 4-9. Total Fuel Consumption based on engine load percentage for case A.

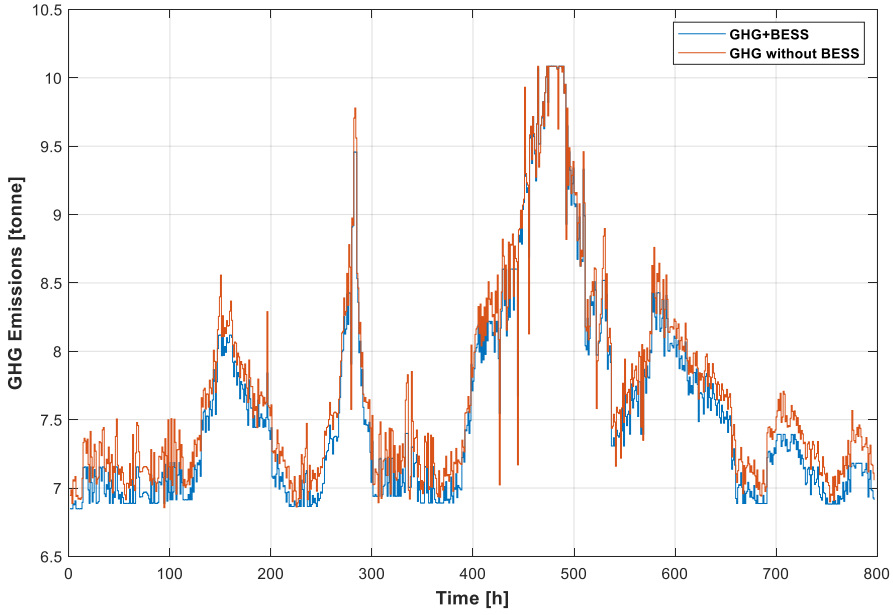

Figure 4-10.Total GHG emissions based on fuel Consumption for case A.

Table 4-3. Comparison of the proposed method in case A

Case A	Operation Cost [$]	Fuel [t]	GHG mass [t]		
			CO2	SOX	NOX
Five generators+BESS	1009543	1715	5470	514	19.8
Five generators	1008205	1750	5595	525	21.8

As a result, by using BESS, the reduction of fuel consumption and GHG emissions are guaranteed, as shown in figures (4-9), (4-10), and Table (4-3). Therefore, batteries are considered a crucial option to compensate for the transient peak power due to sea disturbances and impacts on fuel emissions by reducing the quantity of fuel consumption. Concerning fuel consumption and GHG emissions, the proposed method for five gen-sets included BESS in the present study and compares it in BESS's absence. The results in Table 4-3 show that fuel consumption and GHG emission using BESS and NARX load prediction are roughly 2% reduced compared with five gen-sets factors in a month of operation. This methodology is achieved by creating optimal power reference among DGs and BESS and peak shaving of DGs via PMS in the DP operation. However, the total cost of operation is slightly increased by applying BESS. Still, the fuel consumption is reduced by approximately 35 tonnes per month, by the fuel price of 400 $ per tonne's to pay back the total BESS operation costs.

4.3.2 Case study B: Weekly economic dispatch of generators with BESS based on predicted DP power demand.

The result of Case (b) is evaluated the predicted power demand based on section 3.2.4.2 in hours of the week, and it is investigated the optimization solution in BESS's presence in different sea state sequence with the NARX method. Hence, Figure 4-11 illustrates an optimal problem solution in which PMS is applied suitable strategy to avoid the risk of blackout during the peak load demand due to high DP operation in the period of 80 to 100 hours. The proposed method compensates for generators' oscillations in the presence of BESS in Figure 4-12. Furthermore, Figure 4-13 displays the hourly dispatching of BEES in various DP operations based on MINLP methods to generate optimal power-sharing between gen-sets. Moreover, It has been demonstrated that batteries are charged DGs at their optimum operating points related to the SFOC curve in Figure 4-2 and consume less fuel per unit of energy than conventional electric propulsion settings.

Consequently, Figure 4-14 confirms that the optimal operation point is 188.3[g/kwh], and the maximum efficiency of engine load percentage related to the SFOC surface changes is between 65 to100 percent. In contrast, while BESS is absent, the optimal solution is infeasible. Thus, generators are operated at low efficiency of the SFOC surface where the values are changed between 25 to100 percentage of engine rate as illustrated in Figure 4-15.

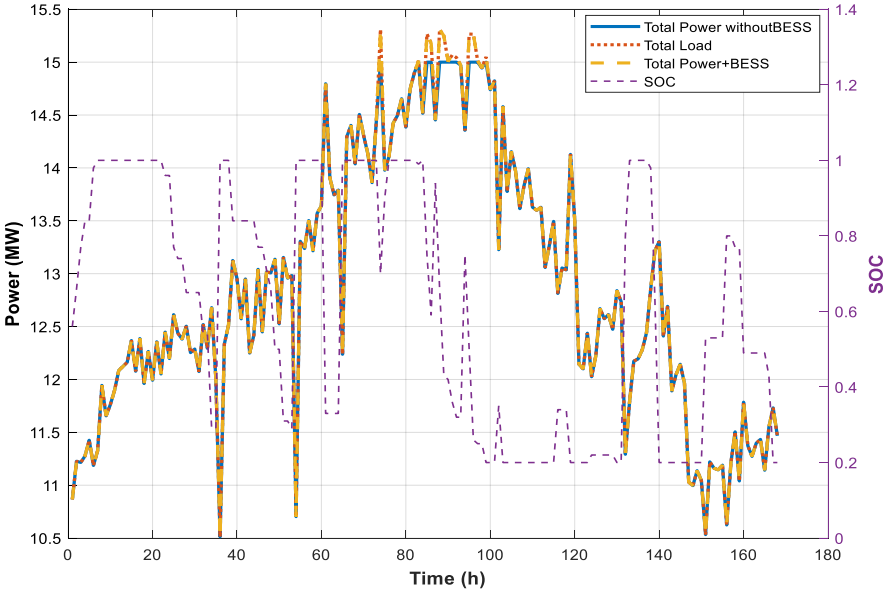

Figure 4-11. Optimal operation of DP ship for different power demands integrated with BESS.

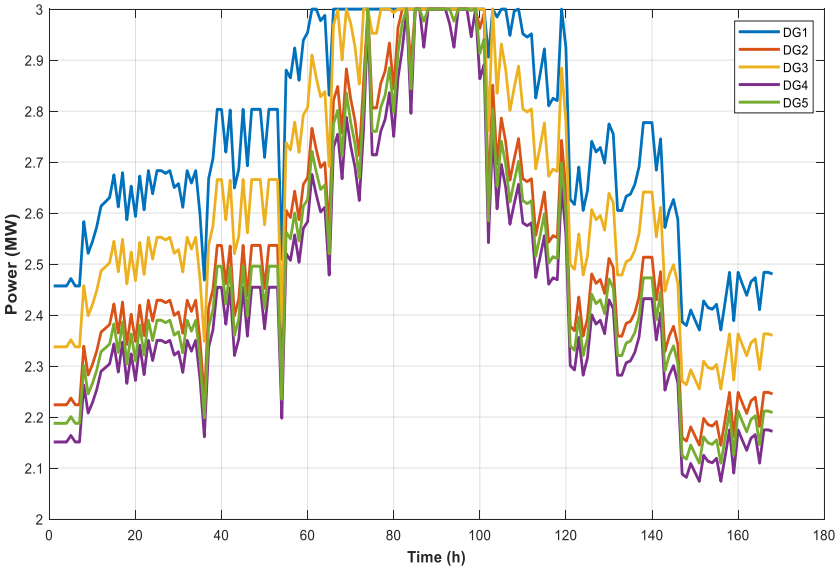

Figure 4-12. Optimal power generation of DGs based on BEES and MINLP methods.

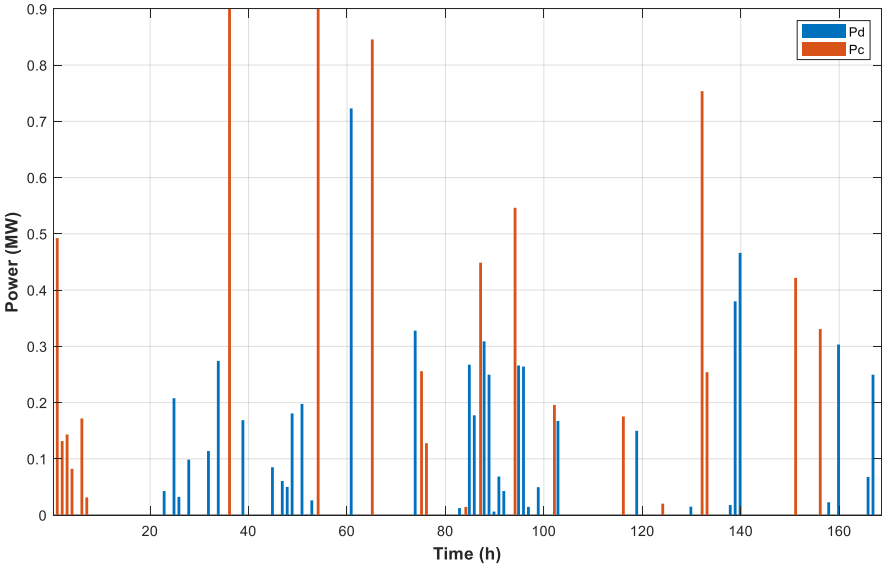

Figure 4-13. The hourly dispatch of BEES based on MINLP methods for different DP operation

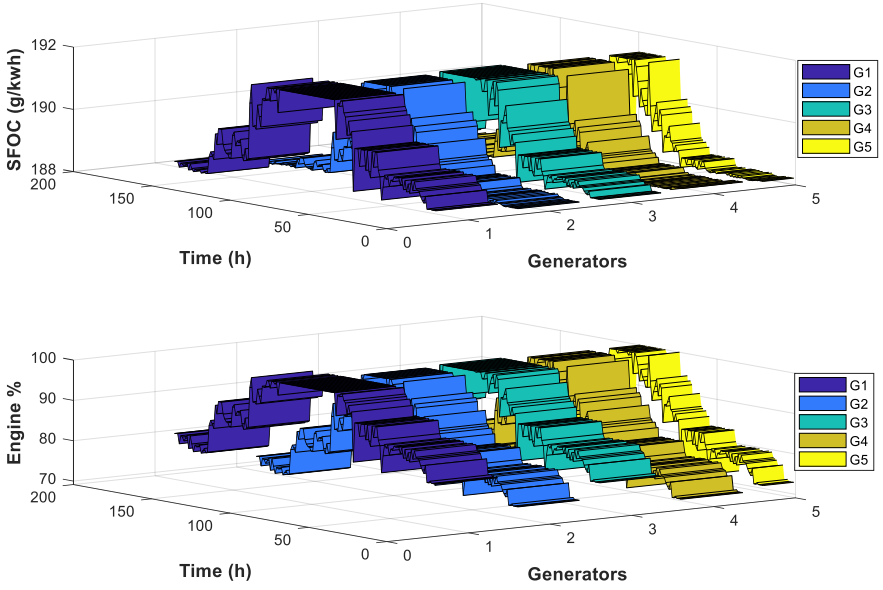

Figure 4-14. The SFOC curve is based on engine loading percentage for five gen-sets with BESS

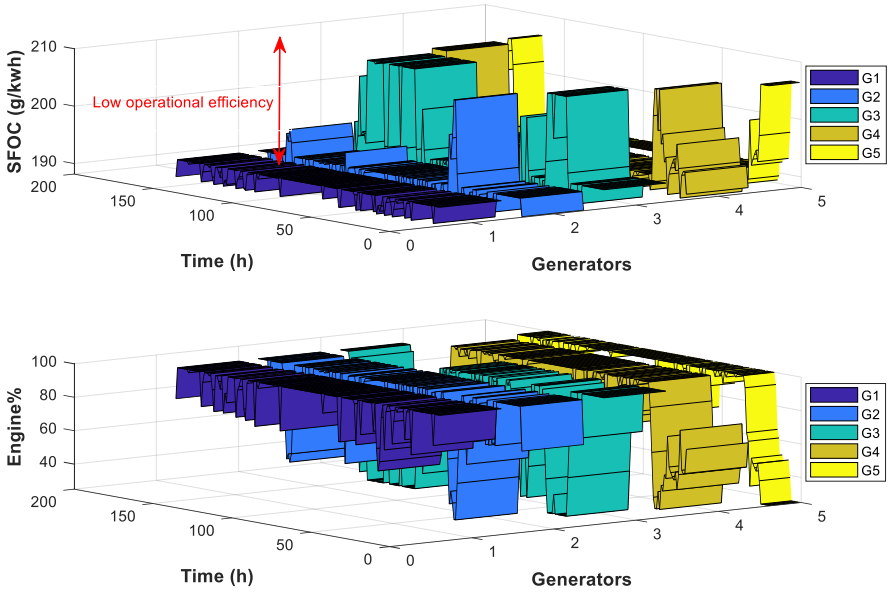

Figure 4-15. The SFOC curve is based on engine loading percentage for five gen-sets without BESS.

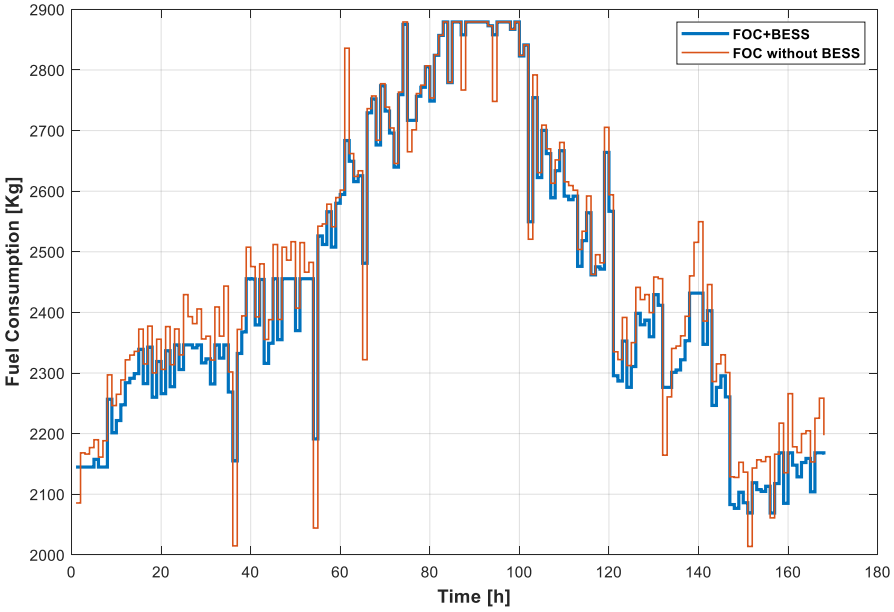

Figure 4-16. Total Fuel Consumption is based on engine load percentage for case B.

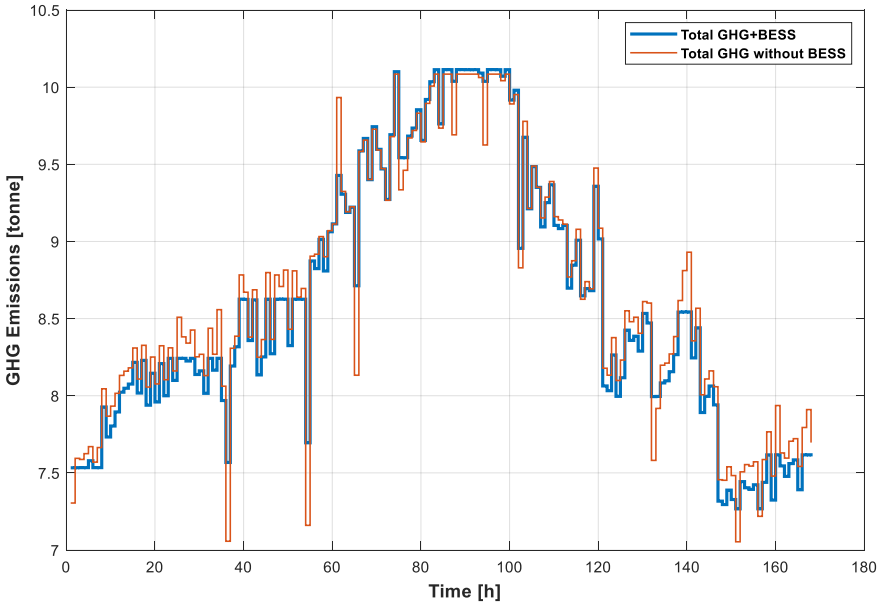

Figure 4-17. Total GHG emissions based on fuel Consumption for case B.

Table 4-4. Comparison of the proposed method in case B

Case B	Operation cost [$]	Fuel[t]	GHG mass [t]		
			CO2	SOX	NOX
Five generators+BESS	215152	409.86	1311.5	122.1	5.1
Five generators	215231	415.01	1323.6	124.5	5.2

As a result, by integrating BESS to AC busbar, the reduction of fuel consumption and GHG emissions are guaranteed as shown in Figures (4-16), (4-17), and Table (4-4). Consequently, batteries are performed a crucial role in compensating for the transient peak power caused by sea disturbances, affecting fuel emissions by reducing the quantity of fuel consumption. Regarding fuel consumption and GHG emissions, the proposed method based on MINLP is involved in BESS operation for a week (168h) in this study and compares it with BESS's absence. The results in Table 4-4 show that fuel consumption and GHG emission by using BESS and NARX–NN load prediction are roughly 1.2% less than compared with five generators factor in a week of operation. This methodology is achieved because of manufacturing optimal power reference among DGs and BESS and peak shaving of DGs via PMS in the DP operation. However, the total cost of operation by applying BESS has been slightly more significant. Still, the GHG mass reduces by approximately 14 [t], and fuel-

saving to 5.2 tonnes per week are guaranteed 400 $ per tonne's fuel price to pay the total BESS operation costs.

4.3.3 Case study C: Operational planning with battery based on Hourly load forecasting in different sea conditions

The case (C) results are assessed based on predicted power demand by the NARX network in BESS in different sea conditions described in section 3.2.4.3. As a result, Figure 4-18 demonstrates an optimal PMS strategy by integrating BESS to avoid the blackout in the peak load in 13 to 18 hours due to high DP operation. While the total generated power could not compensate for the peak demand, BESS power is discharged to the AC busbar as shown in Figures 4-18,4-19 and 4-20 for damping generators power oscillations. Moreover, Figure 4-19 indicates the hourly dispatch of BEES for different DP operations based on MINLP methods to produce optimal power generations between gen-sets.

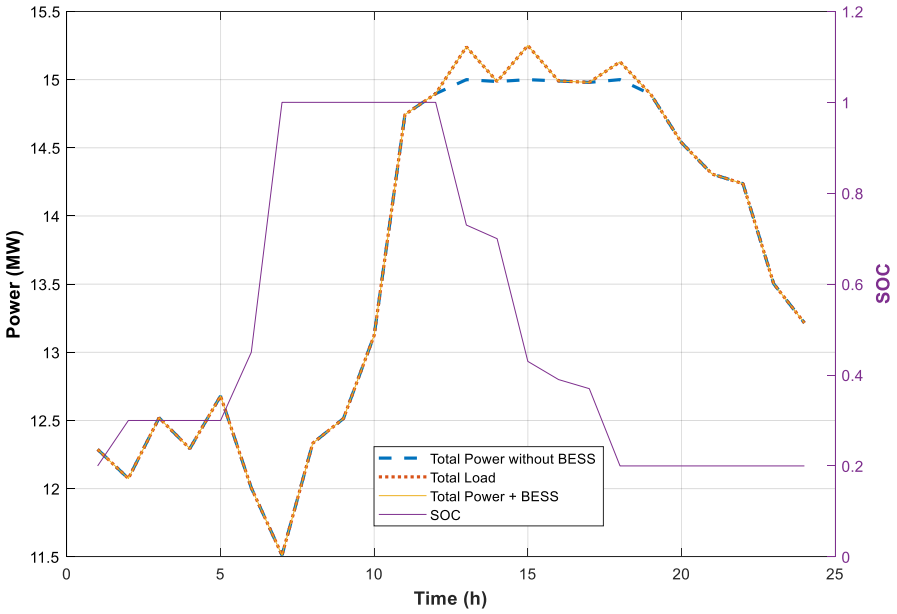

Figure 4-18. Optimal operation of DP ship for different power demand based on BESS.

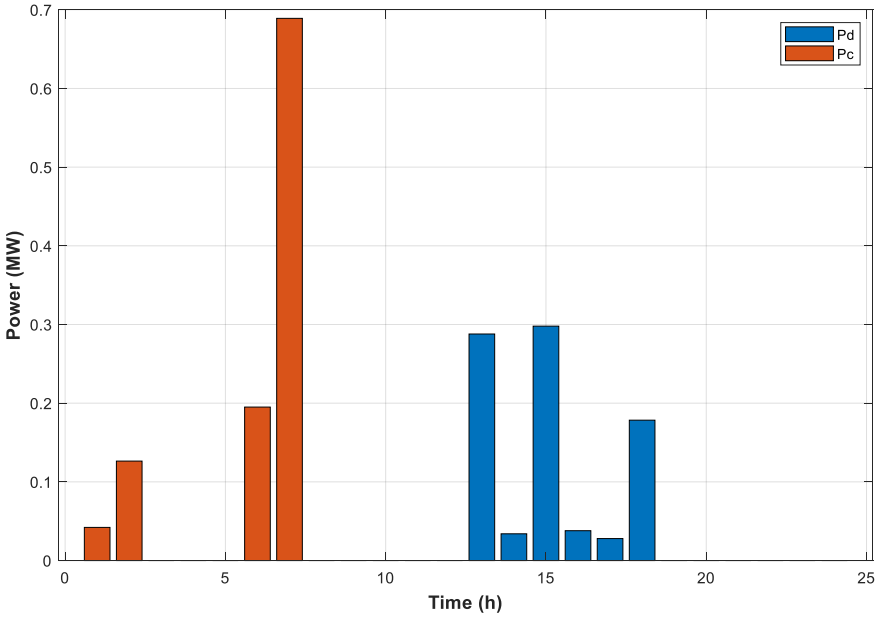

Figure 4-19. The hourly dispatch of BEES is based on MINLP methods for different DP operations.

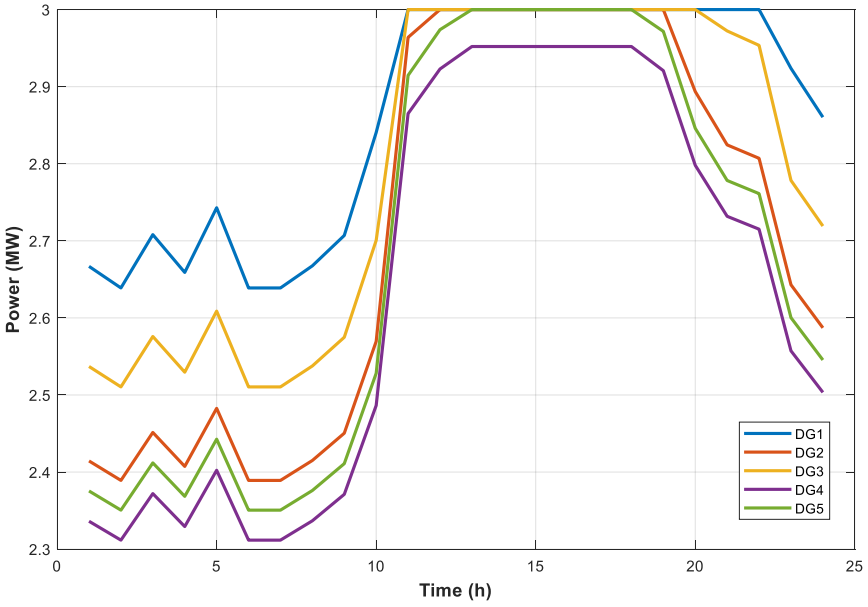

Figure 4-20. Optimal power generation of DGs with BEES and MINLP methods.

Furthermore, it is detected that batteries are charged and discharged power to DGs at their optimal operating point based on SFOC in Figure 4-2. Therefore, BESS is charged while the DPS operates at low power demand and shift the engine operation point to maximum efficiency regions between 77 to100 percent. On the other hand, it discharges during high thruster's command force to consume less fuel per unit of energy than conventional electric propulsion settings.

As a result, Figure 4-21 shows the optimal operation points in 188.3[g/kwh], and the maximum efficiency of engine load percentage is 192[g/kwh] based on SFOC surface, which changes between 77 to100 percent. Meanwhile, in BESS's absences, the optimum solution is infeasible due to inconvenient produced power by generators as presented in Figure 4-22. Hence, generators are operated in the minimum energy efficiency between 190[g/kwh] to 206.5[g/kwh] based on the SFOC surface, which is changed between 25 to100 percent of engines ramp rate as illustrated in Figure 4-23.

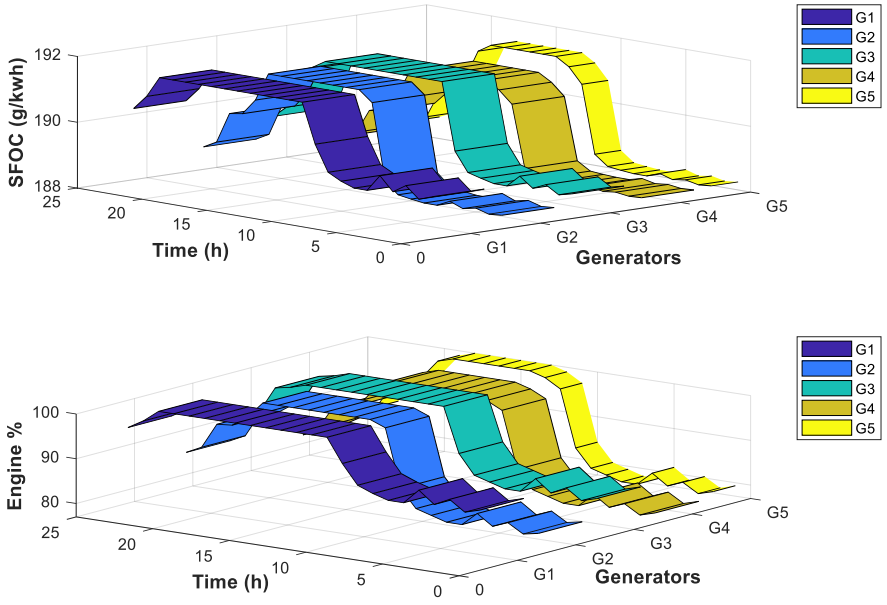

Figure 4-21. The SFOC curve is based on engine loading percentage for five gen-sets with BESS.

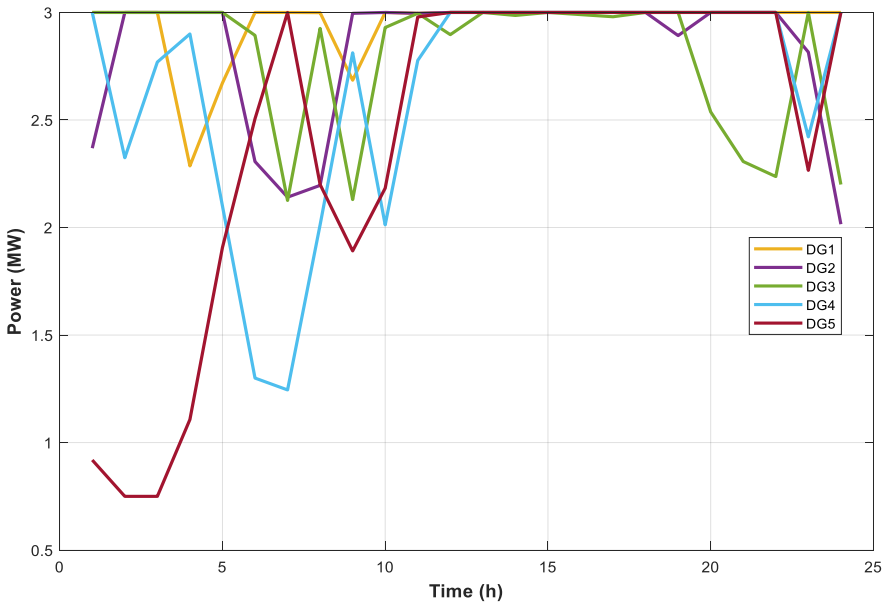

Figure 4-22. Power generation of DGs without BEES and MINLP methods.

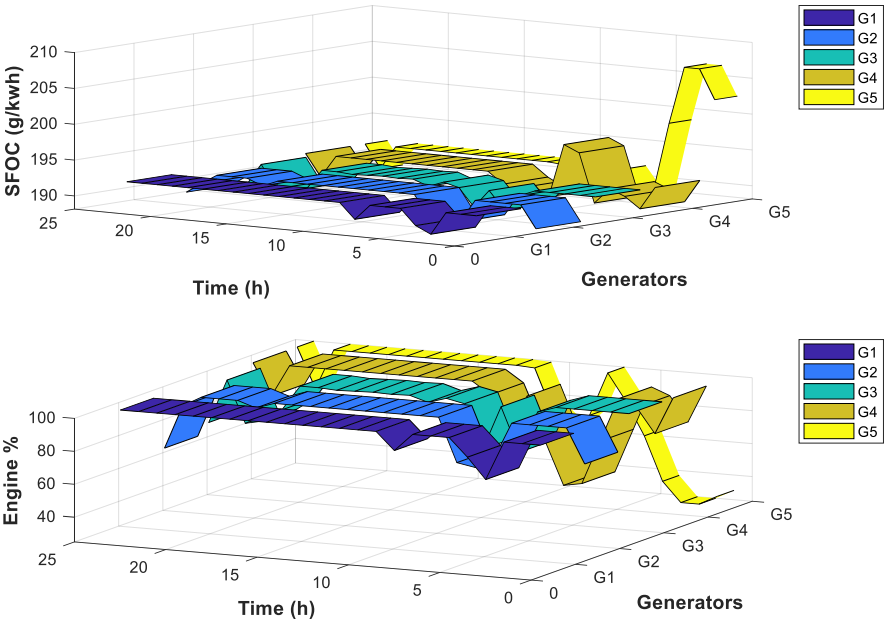

Figure 4-23. The SFOC curve is based on the engine load percentage for five gen-sets without BESS.

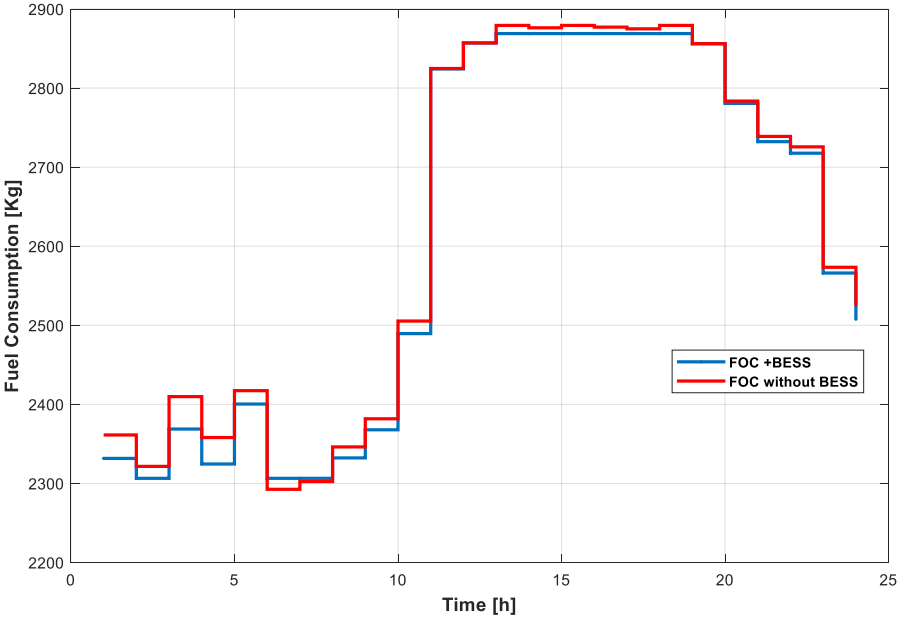

Figure 4-24. Total Fuel Consumption is based on engine load percentage for case C

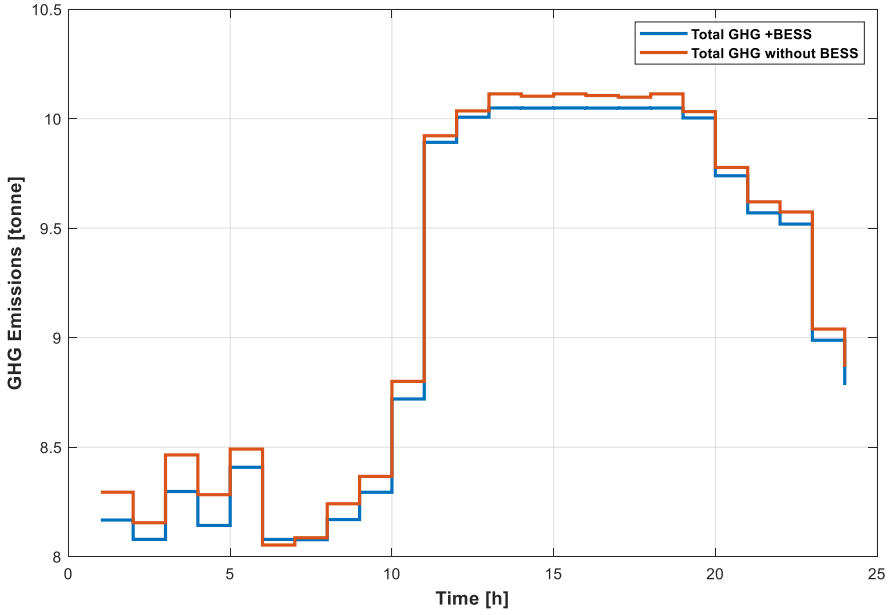

Figure 4-25. Total GHG emissions based on fuel Consumption for case C

Table 4-5. Comparison of the proposed method in case C

Case C	Operation Cost [$]	Fuel [t]	GHG mass [t]		
			CO2	SOX	NOX
Five generators+BESS	30920.97	62.3	199	18.1	0.72
Five generators	30904.47	62.8	200.2	18.7	0.78

As a result, by integrating BESS to AC busbar, the reduction of fuel consumption and GHG emissions are guaranteed as shown in figures (4-24), (4-25), and Table (4-5). Therefore, batteries are executed a critical role in compensating the transient peak power caused by sea disturbances and effects on fuel emissions by reducing the quantity of fuel consumption. Regarding fuel consumption and GHG emissions, the proposed method based on MINLP has involved BESS operation for a day (24h) in this study and compares it with BESS's absence. The results in Table 4-5 show that fuel consumption and GHG emission by using BESS and NARX–NN load prediction is roughly 0.5 [t] less than compared with five generators factor in a day of operation. This methodology is achieved due to producing optimal power reference among DGs and BESS and peak shaving of DGs via PMS in the DP operation. However, the total cost of operation by applying BESS is enhanced. Still, the GHG reduction of approximately one [t] and fuel-saving to 0.8% per day is guaranteed by 400 $ per tonne's fuel price to pay back the total BESS operation costs.

CHAPTER 5. CONCLUSION AND FUTURE REMARKS

Conclusion

This Ph.D. thesis is focused on the PMS strategy for the maritime microgrid. This strategy is used to optimally manage power generations in BESS's presence for reducing GHG emissions and fuel oil consumption of offshore support vessels. A deep learning method is proposed to predict the DP power demand based on sea conditions to cover the objectives. For that reason, the expected power consumption of thrusters is forecasted for the PMS to compensate for the transient power demand in extraordinarily rough and sudden sea state changes. This progressed method enhances operational planning, optimizing engine performance to reduce fuel consumption and GHG emissions based on multi-objective functions that have been solved by nonlinear programming (MINLP) optimization problems. Therefore, this thesis is concluded in the following chapters:

Chapter 1 introduces a general overview of the hybrid DP ship power system, then briefly explains some of PMS's critical issues for economic dispatch and optimal unit power generation commitment during DPS operation in different sea conditions. Finally, it describes the Ph.D. thesis objectives and contributions.

Chapter 2 presents a literature review of different control strategies and DPS architecture to achieve progressive control precision and reduce ship motion due to sea disturbances. Moreover, it is studied the possible DP control methods and comperes the convenience DP controllers with different intelligence techniques to improve the operational safety and performance of the DP ship. Furthermore, this chapter elaborates on the PMS energy and cost efficiency to reduce fuel and GHG emissions in the DP vessels as an essential topic for future research. Hence, the PMS can control the power generations between the DGs and ESS in the DP operation. As a result, DPS's predicted thrusters' power consumption is provided for PMS with an effective optimization method such as the MILP algorithm. Hence, the PMS can be sure of DP demand in the prospect of operation conditions and optimal power generations. The requested DP power could be forecast via PMS based on the AI method and efficient optimization strategy. Consequently, it is essential to produce adequate energy in the shipboard power plants and increase power system stability during the DPS operation. For that reason, an advantaged control strategy is required for PMS to predict the thrusters' power consumption on the shipboard system.

Chapter 3 presents by introducing the AI technology for load forecasting. The proposed method is applied in DPS to predict the thruster’s power consumption as an essential issue in DP ships. Hence, the PMS can be informed from DPS for optimal operation and economically dispatching between generators in different sea conditions. As a result, unpredicted power demand from PMS due to sudden weather changes and the DP operation is forecasted by an intelligent method. Hence, this chapter is introduced a deep learning method based on the NARX for DPS to predict thrusters' power demand for PMS during repositioning accurately. This methodology can help the PMS perform optimal power-sharing between gen-sets and BESS in the complex decision-making process in all kinds of DP ships. Therefore, a recurrent network based on the NARX algorithm is suggested to forecast the STLP of DP power demand. In this method, a precise prediction of the DP power demand compensates for ship motion in sea disturbances. The NARX network delivers the necessary information of the future DP power demand to make better PMS decisions in sea disturbances. Accordingly, a Levenberg-Marquardt (LM-BP) based on the NARX is used to increase the learning process's accuracy in the environmental disturbances as external inputs of the ANN. Thus, this method is used to precisely estimate thrusters' power consumption, known as an environmentally sensitive load in the DP shipboard system. The proposed method is applied to forecast hourly, daily, and in a month of thrusters' power consumption as different scenarios based on sea conditions. As a result, The NARX model is studied on the DP ship model equipped with the thruster control system to keep vessel positioning in different sea conditions. The NARX technique is assessed with the typical time series-NN configurations, where the NARX method confirms considerable accuracy with the other prediction method in sea disturbances.

Chapter 4 introduces the optimization strategy and ESS, which is applied based on predicted DP demand in three different scenarios to increase the power generation system's efficiency. This advantaged method is combined PMS with DPS to exchange a precise data set with each other for improving operational planning of DP ships power plant. Hence, STLP scenarios are defined for load prediction in sea conditions, which can increase PMS accuracy to optimal power-sharing, economic dispatch and reduce fuel consumption during DP operation in the presence of BESS authorization. Furthermore, the generated optimal power setpoints produced by the PMS based on precisely forecasted thrusters power demand with NARX method in different scenarios prevent the risk of shutdown and shave the peak load in the presence of BESS. PMS's produced setpoint is given to the diesel generators (DGs) governor to adjust the network's power and frequency as the local controller. Accordingly, The optimized power references are produced by PMS based on the multi-objective functions by integrating DG and BESS limitations. Finally, To solve the optimization problem, the MINLP algorithm is performed in GAMS software to decrease total fuel consumption and GHG emissions in both DP and drilling operations. As a result, integrating the proposed optimization method and deep learning technique in ESS presence shows that DGs' have the highest performance based on SFOC, minimum fuel consumption, and CO2 emissions during the DP operational condition.

Chapter 5 is summarized the contributions of this thesis.

Future work

- Investigate other ESS such as flywheels, supercapacitors, fuel cells, and shaft generator as the variable speed gen-set can potentially integrate with the existing power generators to increase energy efficiency.
- Development of the DPS controller and PMS program based on python algorithms to execute practically in the real DP ships.

LITERATURE LIST

[1] Q. Shen, B. Ramachandran, S. K. Srivastava, M. Andrus, and D. A. Cartes, “Power and energy management in integrated power system,” *2011 IEEE Electr. Sh. Technol. Symp. ESTS 2011*, pp. 414–419, 2011.

[2] F. Kanellos, A. Anvari-Moghaddam, and J. Guerrero, “Smart Shipboard Power System Operation and Management,” *Inventions*, vol. 1, no. 4, p. 22, 2016.

[3] E. Skjong, T. A. Johansen, M. Molinas, and A. J. Sorensen, “Approaches to Economic Energy Management in Diesel-Electric Marine Vessels,” *IEEE Trans. Transp. Electrif.*, vol. 3, no. 1, pp. 22–35, 2017.

[4] F. D. Kanellos, A. Anvari-Moghaddam, and J. M. Guerrero, “Smart shipboard power system operation and management,” *Inventions*, vol. 1, no. 4, Dec. 2016.

[5] T. Q. Dinh, T. M. N. Bui, J. Marco, C. Watts, and J. I. Yoon, “Optimal Energy Management for Hybrid Electric Dynamic Positioning Vessels,” *IFAC-PapersOnLine*, vol. 51, no. 29, pp. 98–103, 2018.

[6] A. Anvari-Moghaddam, T. Dragicevic, Lexuan Meng, Bo Sun, and J. M. Guerrero, “Optimal planning and operation management of a ship electrical power system with energy storage system,” in *IECON 2016 - 42nd Annual Conference of the IEEE Industrial Electronics Society*, 2016, pp. 2095–2099.

[7] F. Balsamo, P. De Falco, F. Mottola, and M. Pagano, “Power Flow Approach for Modeling Shipboard Power System in Presence of Energy Storage and Energy Management Systems,” *IEEE Trans. Energy Convers.*, vol. 8969, no. c, pp. 1–1, 2020.

[8] M. Othman, A. Anvari-Moghaddam, and J. M. Guerrero, “Hybrid shipboard microgrids: System architectures and energy management aspects,” *Proc. IECON 2017 - 43rd Annu. Conf. IEEE Ind. Electron. Soc.*, pp., 6801–6806, 2017.

[9] F. D. Kanellos, A. Anvari-Moghaddam, and J. M. Guerrero, “A cost-effective and emission-aware power management system for ships with integrated full electric propulsion,” *Electr. Power Syst. Res.*, vol. 150, pp. 63–75, 2017.

[10] R. D. Geertsma, R. R. Negenborn, K. Visser, and J. J. Hopman, “Design and control of hybrid power and propulsion systems for smart ships: A review of developments,” *Appl. Energy*, vol. 194, pp. 30–54, 2017.

[11] M. Mehrzadi, C. Su, Y. Terriche, J. C. Vasquez and J. M. Guerrero, "Operation Planning of Standalone Maritime Power Systems Using Particle Swarm Optimization," *2019 1st International Conference on Electrical, Control and Instrumentation Engineering (ICECIE)*, Kuala Lumpur, Malaysia, 2019, pp. 1-6.

[12] F. Arditti, H. Cozijn, E. F. G. Van Daalen, and E. A. Tannuri, “Dynamic Positioning simulations of a Thrust Allocation Algorithm considering Hydrodynamic Interactions,” *IFAC-PapersOnLine*, vol. 51, no. 29, pp. 122–

127, Jan. 2018.
[13] M. Mehrzadi, Y. Terriche, C. L. Su, M. Bin Othman, J. C. Vasquez, and J. M. Guerrero, "Review of dynamic positioning control in maritime microgrid systems," *Energies*, vol. 13, no. 12, pp. 1–22, 2020.
[14] T. I. Fossen, "A survey on Nonlinear Ship Control: from Theory to Practice," *IFAC Proc. Vol.*, vol. 33, no. 21, pp. 1–16, Aug. 2000.
[15] A. J. Sørensen, "A survey of dynamic positioning control systems," *Annu. Rev. Control*, vol. 35, no. 1, pp. 123–136, 2011.
[16] J. G. Balchen, N. A. Jenssen, E. Mathisen, and S. Sælid, "A Dynamic Positioning System Based on Kalman Filtering and Optimal Control," *Model. Identif. Control A Nor. Res. Bull.*, vol. 1, no. 3, pp. 135–163, 1980.
[17] M. J. Grimble, R. J. Patton, and D. A. Wise, "Use of Kalman filtering techniques in dynamic ship-positioning systems," *IEE Proc. D Control Theory Appl.*, vol. 127, no. 3, p. 93, 1980.
[18] S. Saelid, J. G. Balchen, and N. A. Jenssen, "Design and Analysis of a Dynamic Positioning System Based on Kalman Filtering and Optimal Control," *IEEE Trans. Automat. Contr.*, vol. 28, no. 3, pp. 331–339, 1983.
[19] "Kalman filtering for positioning and heading control of ships and offshore rigs," *IEEE Control Syst.*, vol. 29, no. 6, pp. 32–46, Dec. 2009.
[20] J. Balchen, N. Jenssen, E. Mathisen, and S. Saelid, "Dynamic positioning of floating vessles based on Kalman filtering and optimal control," in *1980 19th IEEE Conference on Decision and Control including the Symposium on Adaptive Processes*, 1980, pp. 852–864.
[21] A. J. Sørensen, "A survey of dynamic positioning control systems," *Annu. Rev. Control*, vol. 35, no. 1, pp. 123–136, 2011.
[22] Fossen, T.I.; Grovlen, A. Nonlinear output feedback control of dynamically positioned ships using vectorial observer backstepping. IEEE Trans. Control Syst. Technol. 1998, 6, 121–128.
[23] X. Hu, J. Du, and J. Shi, "Adaptive fuzzy controller design for dynamic positioning system of vessels," *Appl. Ocean Res.*, vol. 53, pp. 46–53, Oct. 2015.
[24] S. S. Ge and C. Wang, "Adaptive Neural Control of Uncertain MIMO Nonlinear Systems," *IEEE Trans. Neural Networks*, vol. 15, no. 3, pp. 674–692, May 2004.
[25] M.-C. Fang and Z.-Y. Lee, "Application of neuro-fuzzy algorithm to portable dynamic positioning control system for ships," *Int. J. Nav. Archit. Ocean Eng.*, vol. 8, no. 1, pp. 38–52, Jan. 2016.
[26] Y. Li, S. Tong, and T. Li, "Adaptive fuzzy output feedback control of nonlinear uncertain systems with unknown backlash-like hysteresis based on modular design," *Neural Comput. Appl.*, vol. 23, no. S1, pp. 261–270, Dec. 2013.
[27] S. C. Tong, Y. M. Li, and H.-G. Zhang, "Adaptive Neural Network Decentralized Backstepping Output-Feedback Control for Nonlinear Large-Scale Systems with Time Delays," *IEEE Trans. NEURAL NETWORKS*, vol. 22, no. 7, p. 1073, 2011.
[28] T. D. Nguyen, A. J. Sørensen, and S. Tong Quek, "Design of hybrid controller

for dynamic positioning from calm to extreme sea conditions," *Automatica*, vol. 43, no. 5, pp. 768–785, May 2007.

[29] A. R. Dahl, L. Thorat, and R. Skjetne, "Model Predictive Control of Marine Vessel Power System by Use of Structure Preserving Model," *IFAC-PapersOnLine*, vol. 51, no. 29, pp. 335–340, 2018.

[30] M. V. Sotnikova and E. I. Veremey, "Dynamic Positioning Based on Nonlinear MPC," *IFAC Proc. Vol.*, vol. 46, no. 33, pp. 37–42, Jan. 2013.

[31] H. Chen, L. Wan, F. Wang, and G. Zhang, "Model predictive controller design for the dynamic positioning system of a semi-submersible platform," *J. Mar. Sci. Appl.*, vol. 11, no. 3, pp. 361–367, Sep. 2012.

[32] A. Veksler, T. A. Johansen, F. Borrelli, and B. Realfsen, "Dynamic Positioning With Model Predictive Control," *IEEE Trans. Control Syst. Technol.*, vol. 24, no. 4, pp. 1340–1353, Jul. 2016.

[33] T. I. Bø, T. A. Johansen, A. J. Sørensen, and E. Mathiesen, "Dynamic consequence analysis of marine electric power plant in dynamic positioning," *Appl. Ocean Res.*, vol. 57, pp. 30–39, 2016.

[34] T. A. Johansen, T. I. Bo, E. Mathiesen, A. Veksler, and A. J. Sorensen, "Dynamic Positioning System as Dynamic Energy Storage on Diesel-Electric Ships," IEEE Trans. Power Syst., vol. 29, no. 6, pp. 3086–3091, Nov. 2014.

[35] Veksler, A.; Johansen, T.A.; Skjetne, R.; Mathiesen, E. Reducing power transients in diesel-electric dynamically positioned ships using re-positioning. In Proceedings of the IEEE IECON Conference, Dallas, TX, USA, 29 October–1 November 2014; pp. 268–273.

[36] A. Veksler, T. A. Johansen, and R. Skjetne, "Transient power control in dynamic positioning - Governor feedforward and dynamic thrust allocation," in *IFAC Proceedings Volumes (IFAC-PapersOnline)*, Sep.2012, vol. 9, no.1, pp. 158–163.

[37] F. Arditti, H. Cozijn, E. F. G. Van Daalen, and E. A. Tannuri, "Dynamic Positioning simulations of a Thrust Allocation Algorithm considering Hydrodynamic Interactions," *IFAC-PapersOnLine*, vol. 51, no. 29, pp. 122–127, Jan. 2018.

[38] M. Mehrzadi *et al.*, "A Deep Learning Method for Short-Term Dynamic Positioning Load Forecasting in Maritime Microgrids," *Appl. Sci.*, vol. 10, no. 14, p. 4889, Jul. 2020.

[39] A. Veksler, T. A. Johansen, R. Skjetne, and E. Mathiesen, "Thrust Allocation With Dynamic Power Consumption Modulation for Diesel-Electric Ships," *IEEE Trans. Control Syst. Technol.*, vol. 24, no. 2, pp. 578-593, March 2016.

[40] A. Veksler, T. A. Johansen, and R. Skjetne, "Thrust allocation with power management functionality on dynamically positioned vessels," *American Control Conference (ACC).*, pp. 1468–1475, June. 2012.

[41] Z. X. Xiao *et al.*, "Operation Control for Improving Energy Efficiency of Shipboard Microgrid including Bow Thrusters and Hybrid Energy Storages," *IEEE Trans. Transp. Electrif.*, vol. 6, no. 2, pp. 856–868, 2020.

[42] A. J. Sorensen *et al.*, "Toward Safer, Smarter, and Greener Ships: Using Hybrid Marine Power Plants," *IEEE Electrif. Mag.*, vol. 5, no. 3, pp. 68–73, 2017.

[43] D. Radan, T. A. Johansen, A. J. Sørensen, and A. K. Ådnanes, "Optimization of load-dependent start tables in marine power management systems with blackout prevention," *WSEAS Trans. Circuits Syst.*, vol. 4, no. 12, pp. 1861–1866, 2005.

[44] S. K. Sheikh and M. G. Unde "Short-term load forecasting using ANN technique," Int. J. Eng. Sci. Emerg. Technol., vol. 1, no. 2, pp: 97-107,2012.

[45] H. M. Al-Hamadi and S. A. Soliman, "Long-term/mid-term electric load forecasting based on short-term correlation and annual growth," *Electr. Power Syst. Res.*, vol. 74, no. 3, pp. 353–361, Jun. 2005.

[46] K. Y. Lee, Y. T. Cha, and J. H. Park, "Short-term load forecasting using an artificial neural network," *IEEE Trans. Power Syst.*, vol. 7, no. 1, pp. 124–132, 1992.

[47] H. Quan, D. Srinivasan, and A. Khosravi, "Short-term load and wind power forecasting using neural network-based prediction intervals," *IEEE Trans. Neural Networks Learn. Syst.*, vol. 25, no. 2, pp. 303–315, Feb. 2014.

[48] Y. Wu, "Short-term forecasting for distribution feeder loads with consumer classification and weather dependent regression," *IEEE Lausanne Power Tech*, pp. 689–694, July 2007.

[49] A. Garulli, S. Paoletti, and A. Vicino, "Models and Techniques for Electric Load Forecasting in the Presence of Demand Response," *IEEE Trans. Control Syst. Technol.*, vol. 23, no. 3, pp. 1087–1097, May 2015.

[50] E. A. Feilat and M. Bouzguenda, "Medium-term load forecasting using neural network approach," in 2011 *IEEE* PES Conference on Innovative Smart Grid Technologies - Middle East, ISGT Middle East 2011, 2011.

[51] V. N. Coelho, F. G. Guimaraes, A. J. R. Reis, I. M. Coelho, B. N. Coelho, and M. J. F. Souza, "A heuristic fuzzy algorithm bio-inspired by Evolution Strategies for energy forecasting problems," in *IEEE International Conference on Fuzzy Systems*, pp. 338–345, 2014.

[52] R. J. Wai, Y. C. Huang, and Y. C. Chen, "Intelligent daily load forecasting with fuzzy neural network and particle swarm optimization," in *IEEE International Conference on Fuzzy Systems, IEEE*, pp. 1-6, Aug 2012.

[53] H. B. Azad, S. Mekhilef, and V. G. Ganapathy, "Long-term wind speed forecasting and general pattern recognition using neural networks," *IEEE Trans. Sustain. Energy*, vol. 5, no. 2, pp. 546–553, Apr. 2014.

[54] S. S. Soman, H. Zareipour, O. Malik, and P. Mandal, "A review of wind power and wind speed forecasting methods with different time horizons," in North American Power Symposium 2010.*IEEE*, pp.1-8, Aug 2010.

[55] D. Fay, J. V Ringwood, and S. Member, "On the Influence of Weather Forecast Errors in Short-Term Load Forecasting Models," *IEEE Trans* on Power Systems, vol. 25, no. 3, pp. 1751–1758, 2010.

[56] M. J. Willis, G. A. Montague, C. Di Massimo, M. T. Tham, and A. J. Morris, "Artificial neural networks in process estimation and control," *Automatica*, vol. 28, no. 6, pp. 1181–1187, Nov. 1992.

[57] K. J. Hunt, D. Sbarbaro, R. Zbikowski, and P. J. Gawthrop, "Neural networks for control systems-A survey," *Automatica*, vol. 28, no. 6, pp. 1083–1112, Nov. 1992.

[58] M. R. Habibi, H. R. Baghaee, T. Dragicevic, and F. Blaabjerg, "Detection of False Data Injection Cyber-Attacks in DC Microgrids based on Recurrent Neural Networks," *IEEE J. Emerg. Sel. Top. Power Electron.*, pp. 1–1, Jan. 2020.

[59] H. T. Siegelmann, B. G. Horne, and C. L. Giles, "Computational capabilities of recurrent NARX neural networks," *IEEE Trans. Syst. Man, Cybern. Part B Cybern.*, vol. 27, no. 2, pp. 208–215, 1997.

[60] S. Mandal and N. Prabaharan, "Ocean wave forecasting using recurrent neural networks," Ocean engineering, vol. 33, pp. 1401–1410, 2006.

[61] J. Schmidhuber, "Deep learning in neural networks: An overview," *Neural Networks*, vol. 61, pp. 85–117, Jan. 2015.

[62] "Deep Learning Toolbox - MATLAB." [Online]. Available: https://se.mathworks.com/products/deep-learning.html. [Accessed: 04-Dec-2020].

[63] M. R. Miyazaki, A. J. Sørensen, and B. J. Vartdal, "Hybrid marine power plants model validation with strategic loading," *IFAC-PapersOnLine*, vol. 49, no. 23, pp. 400–407, 2016.

[64] O. Mo and G. Guidi, "Design of Minimum Fuel Consumption Energy Management Strategy for Hybrid Marine Vessels with Multiple Diesel Engine Generators and Energy Storage," *2018 IEEE Transp. Electrif. Conf. Expo, ITEC 2018*, pp. 537–544, 2018.

[65] H. E. Lindstad, G. S. Eskeland, and A. Rialland, "Batteries in offshore support vessels – Pollution, climate impact and economics," *Transp. Res. Part D Transp. Environ.*, vol. 50, pp. 409–417, 2017.

[66] N. K. Paliwal, A. K. Singh, N. K. Singh, and P. Kumar, "Optimal sizing and operation of battery storage for economic operation of hybrid power system using artificial bee colony algorithm," *Int. Trans. Electr. Energy Syst.*, vol. 29, no. 1, pp. 1–23, 2019.

[67] R. Barrera-Cardenas, O. Mo, and G. Guidi, "Optimal Sizing of Battery Energy Storage Systems for Hybrid Marine Power Systems," *2019 IEEE Electr. Sh. Technol. Symp. ESTS 2019*, pp. 293–302, Aug.2019.

[68] I. Georgescu, M. Godjevac, and K. Visser, "Efficiency constraints of energy storage for on-board power systems," Ocean Eng., vol. 162, pp. 239–247, Aug. 2018.

[69] M. D. A. Al-Falahi, K. S. Nimma, S. D. G. Jayasinghe, H. Enshaei, and J. M. Guerrero, "Power management optimization of hybrid power systems in electric ferries," *Energy Convers. Manag.*, vol. 172, pp. 50–66, Sep. 2018.

[70] A. Soroudi, "Power system optimization modeling in GAMS," Springer International Publishing," Aug 2017.

[71] C. A. Morales Vásquez, "Evaluation of Medium Speed Diesel generator sets and energy storage technologies as alternatives for reducing fuel consumption and exhaust emissions in electric propulsion systems for PSVs," *Cienc. y Tecnol. buques*, vol. 9, no. 18, p. 49, 2016.

APPENDIX. PAPERS

ISSN (online): 2446-1636
ISBN (online): 978-87-7210-861-2 AALBORG UNIVERSITY PRESS